positions of 2α and 2β become farther away from being symmetrical with respect to the C=C—C=O plane, and the orientation of the methylene group at C_2 makes a different angle with the π orbital of the C=O group. Thus the difference in the $\delta(^1H)$ of the protons 2α and 2β are expected to increase and the magnitude of $^2J_{HH}$ of protons 2 will decrease. Indeed, the difference of $\delta(^1H)$ of 2α and 2β was found to be 0.2 ppm and $^2J_{HH}$ decreases markedly to 15.4 Hz.[33] Although the changes associated with protons at position 2 are small, together with the upfield shift of $\delta(^1H)$ of protons 1, they suggest that *in solution*, an inverted conformation or a conformation similar to that found in crystal for the A ring is the predominant one for **1**. One has to be cautious in making conclusions based on proton chemical shifts which are dependent on solvent and anisotropy. However, the present results are consistent with the notion that steroid conformations are usually unchanged between crystal and solution states.

(33) This decrease in $^2J_{HH}$ of H_2 and its conformational implications are firmly substantiated by a separate study in which $^2J_{HH}$ for a series of substituted progesterones, including **1**, were selectively measured via an indirect *J* spectroscopy with much higher accuracy (Wong, T. C.; Clark, G. R. *J. Chem. Soc., Chem. Commun.*, in press). The change of $^2J_{HH}$ of H_2 was found to agree perfectly with theoretical predictions (ref 31) based on structures determined from X-ray diffraction.

Conclusion

This study of a relatively complex molecule **1** demonstrates again that indirect homonuclear decoupling gives rise to useful ^1H–^{13}C chemical shift correlation maps. Measurements of ^1H chemical shifts, geminal couplings $^2J_{HH}$, and heteronuclear couplings with the additional spin support our opinion that the described 2-D NMR technique provides more pertinent information than the traditional versions of heteronuclear chemical shift correlation.

Acknowledgment. The NT-300 spectrometer was purchased partially through a grant from the National Science Foundation (PCM-8115599). This work is partially supported by the National Institutes of Health Institutional Biomedical Research Support Grant RR07053. Helpful discussion with Dr. Elmer Schlemper is gratefully acknowledged.

Registry No. 1, 127-31-1; **2**, 600-57-7; **3**, 71-58-9; **4**, 57-83-0; 2-fluoropyridine, 372-48-5; 2,5-difluoroaniline, 367-30-6; 1,2-difluorobenzene, 367-11-3; 1,3-difluorobenzene, 372-18-9; 1,4-difluorobenzene, 540-36-3.

Carbon Monoxide Activation by Organoactinides. A Comparative Synthetic, Thermodynamic, Kinetic, and Mechanistic Investigation of Migratory CO Insertion into Actinide–Carbon and Actinide–Hydrogen Bonds To Yield η^2-Acyls and η^2-Formyls

Kenneth G. Moloy and Tobin J. Marks*

Contribution from the Department of Chemistry, Northwestern University, Evanston, Illinois 60201. *Received April 5, 1984*

Abstract: This paper reports the synthesis, characterization, and carbon monoxide chemistry of a series of sterically hindered thorium alkyls and hydrides of the type $Cp'_2Th(R)(X)$ ($Cp' = \eta^5$-C_5Me_5) where R = H, D, Me, *n*-Bu, and CH_2-*t*-Bu and X = OCH-*t*-Bu_2, OC_6H_3-2,6-*t*-Bu_2, and O-*t*-Bu. In addition, improved syntheses of the known complexes $[Cp'_2Th(\mu\text{-}H)(H)]_2$, $Cp'_2Th(O\text{-}t\text{-}Bu)(Cl)$ and $Cp'_2Th(CH_2\text{-}t\text{-}Bu)(Cl)$ are presented. The alkyl complexes undergo facile, irreversible carbonylation to yield η^2-acyls that were characterized by a variety of methods. Infrared and ^{13}C NMR spectra of these complexes demonstrate that strong metal–(acyl)oxygen bonding takes place, fostering a pronounced carbene-like character. Thus, these complexes are characterized by low C–O infrared stretching frequencies (ν_{CO} = 1450–1480 cm^{-1}) and low-field ^{13}C NMR chemical shifts ($\delta_{^{13}C}$ 355–370). The hydrides undergo a rapid, reversible, migratory CO insertion to yield formyls that have been characterized spectroscopically at low temperature. Infrared and ^{13}C NMR spectra of these species are quite similar to the corresponding acyls, suggesting an analogous η^2 structure. Variable-temperature equilibrium data show that the insertion of CO into thorium–hydrogen bonds is exothermic by ca. 5 kcal/mol, and this value is compared to that for the analogous alkyls. The equilibrium was also found to exhibit a distinct equilibrium isotope effect upon deuterium substitution, K_H/K_D = 0.31 at −78 °C. The carbonylation of the complex $Cp'_2Th(n\text{-}Bu)(OCH\text{-}t\text{-}Bu_2)$ was found to obey a second-order rate law where rate = kP_{CO}[complex]. Likewise, the insertion of CO into the Th–H bond of $Cp'_2Th(H)(OCH\text{-}t\text{-}Bu_2)$ was found by NMR methods to be first order in metal hydride. Labeling and crossover experiments offer further support for an intramolecular pathway for CO insertion, resulting in the formation of monomeric formyls. The insertion exhibits a primary kinetic isotope effect; at −54 °C, $(k_H/k_D)_{forward}$ = 2.8 (4) (insertion) and $(k_H/k_D)_{reverse}$ = 4.1 (5) (extrusion). Thus, the insertion is inferred to involve rate-determining migration of the hydride ligand. Approximate rate data for the series of alkyls synthesized show that the rate of hydride migration greatly exceeds that of alkyl migration. For the complexes reported herein, $k(H) \approx 5 \times 10^3 k(CH_2\text{-}t\text{-}Bu) \approx 7 \times 10^4 k(n\text{-}Bu) \approx 10^8 k(Me)$. The latter three rates partially mirror Th–C bond disruption enthalpy trends. The rate of migratory insertion is impeded when the steric bulk of the alkoxide coligand is increased and accelerated when it is replaced by chloride.

One of the most well-studied and important reactions in all of inorganic/organometallic chemistry involves the migratory insertion of carbon monoxide into a metal–alkyl bond to yield an acyl complex (eq 1).[1] Transformations such as this have enormous

0002-7863/84/1506-7051$01.50/0

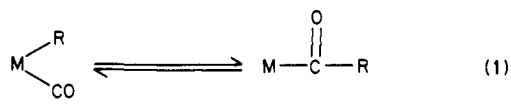

(1)

significance in both stoichiometric and catalytic chemistry.[2] For example, a great many industrial processes involving homogeneous carbon monoxide reduction (e.g., hydroformylation, alcohol synthesis, acetic acid synthesis, etc.) have been proposed to include the insertion depicted in eq 1 as a key, integral step in the catalytic cycle. Considerably less well understood but of conceivably equal importance is the analogous insertion of CO into a metal–hydrogen bond to yield a formyl (R = H in eq 1).[3] A priori, this process is a plausible pathway any time a metal hydride (surface-bound or homogeneous) is involved in the stoichiometric or catalytic reduction of carbon monoxide. However, to date this reaction has been directly observed in homogeneous solution in only two instances. In a recent communication,[4] we reported that thorium hydrides of the type $Cp'_2Th(H)(OR)$ ($Cp' = \eta^5$-C_5Me_5; OR = very bulky alkoxide) undergo a rapid, reversible migratory insertion of carbon monoxide to yield η^2-formyls (eq 2). The pronounced

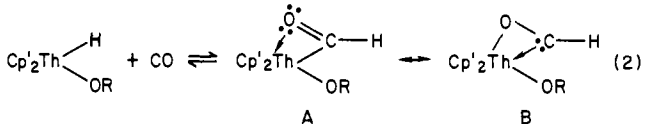

(2)

A B

oxophilicity of thorium[5] is likely a major factor in promoting the "carbene-like" character (B) of the resulting η^2 formyls as well as the favorable position ($\Delta G < 0$) of equilibrium 2. We have previously shown that this oxophilicity-based strategy could be employed for the synthesis of η^2-carbamoyls from thorium and uranium dialkylamides, representing the first examples of CO insertion into metal–nitrogen bonds.[6] Wayland has demonstrated that the rhodium hydrides shown in eq 3 also undergo reversible carbonylation to yield isolable formyls.[7] The mechanism of this reaction is not, however, believed[7] to involve a classical migratory insertion such as that depicted in eq 1.

$$Rh(por)(H) + CO \rightleftharpoons Rh(por)(CHO) \quad (3)$$

por = 1,2,3,4,5,6,7,8-octaethylporphyrin, *meso*-tetraphenylporphyrin

Although the carbonylation of metal hydrides does not in general provide a synthetically viable route to formyl complexes, such species are now accessible by alternative routes. By far the most common of these involves nucleophilic bimolecular hydride transfer to coordinated carbon monoxide (e.g., eq 4).[8] However,

$$L_xM^n\text{–}CO + R_3BH^- \rightarrow L_xM^{n-1}\text{–}CHO + R_3B \quad (4)$$

many formyls thus synthesized undergo rapid decarbonylation (migratory extrusion) to yield the corresponding carbonyl hydride (radical chain decomposition mechanisms have also been identified[8i,j]), suggesting that for most transition metals, the hydride/formyl equilibrium lies far toward the left in eq 1.[8] This thermodynamic instability of metal formyls has led other workers to explore routes by which a formyl fragment might be stabilized through interaction with multiple metal centers (e.g., eq 5[9] and 6[10]). These examples provide further evidence that formyls or μ-CHO fragments may be stabilized via conjunctive metal–oxygen and –carbon bonding.[11]

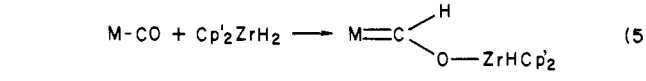

(5)

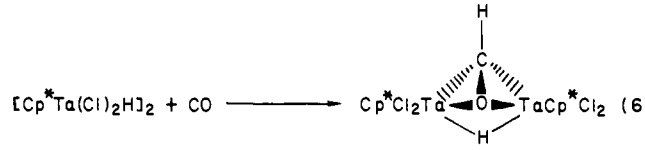

(6)

Cp* = η^5-C_5Me_4Et

Because the carbonylation of thorium hydrides (eq 2) provides the only unequivocal example to date of a simple migratory insertion to yield a mononuclear formyl, a unique opportunity is provided to investigate the thermodynamic, kinetic, and mechanistic aspects of this important process. Moreover, the opportunity now exists to compare and contrast the behavior with that of the analogous alkyls. In the present contribution, we present a complete discussion of our work on this problem. This includes the thermodynamic and kinetic parameters describing eq 2, information on the molecularity of the insertion process, the first measurements of thermodynamic and kinetic isotope effects (ThH vs. ThD) for CO insertion into a metal–hydrogen bond, and the first quantitative comparison of migratory insertion rates for a metal hydride vs. the corresponding metal alkyls (M–R, where R = Me, *n*-Bu, CH_2-*t*-Bu). In the process we also describe improved synthetic methodology for the organoactinides $[Cp'_2Th(\mu\text{-}H)(H)]_2$, $Cp'_2Th(O\text{-}t\text{-}Bu)(Cl)$, and $Cp'_2Th(CH_2\text{-}t\text{-}Bu)(Cl)$.

Experimental Section

Physical and Analytical Measurements. Proton and carbon NMR spectra were recorded on either a Varian EM-390 (CW, 90 MHz), a JEOL FX-90Q (FT, 90 MHz), or a JEOL FX-270 (FT, 270 MHz)

(1) (a) Wojcicki, A. *Adv. Organomet. Chem.* **1973**, *11*, 87–145. (b) Calderazzo, F. *Angew. Chem., Int. Ed. Engl.* **1977**, *16*, 299–311. (c) Kuhlmann, E. J.; Alexander, J. J. *Coord. Chem. Rev.* **1980**, *33*, 195–225. (d) Collman, H. P.; Hegedus, L. S. "Principles and Applications of Organotransition Metal Chemistry"; University Science Books: Mill Valley, CA, 1980.

(2) (a) Biloen, P.; Sachtler, W. M. H. *Adv. Catal.* **1981**, *30*, 165–216. (b) Kung, H. *Catal. Rev.—Sci. Eng.* **1980**, *22*, 235–259. (c) Muetterties, E. L.; Stein, J. *Chem. Rev.* **1979**, *79*, 479–490. (d) Masters, C. *Adv. Organomet. Chem.* **1979**, *17*, 61–103. (e) Ponec, V. *Catal. Rev.-Sci. Eng.* **1978**, *18*, 151–171. (f) Klier, K. *Adv. Catal.* **1982**, *31*, 243–313.

(3) (a) Dombek, B. D. *Adv. Catal.* **1983**, *32*, 326–416. (b) Dombek, B. D. *J. Am. Chem. Soc.* **1980**, *102*, 6855–6857. (c) Hindermann, J. P.; Deluarche, A.; Kieffer, R.; Kiennemann, A. *Can. J. Chem. Eng.* **1983**, *61*, 21–28. (d) Deluzarche, A.; Hindermann, J. P.; Kieffer, R.; Cressely, J.; Stupfler, R.; Kiennemann, A. *Spectra 2000* **1982**, *75*, 27–36. (e) Costa, L. C. *Catal. Rev.—Sci. Eng.* **1983**, *25*, 325–363. (f) Keim, K.-H.; Korff, J.; Keim, W.; Roper, M. *Erdöl Kohle, Erdgas, Petrochem.* **1982**, *35*, 297–304. (g) Feder, H. M.; Rathke, J. W.; Chen, M. J.; Curtiss, L. A. *ACS Symp. Ser.* **1981**, *No. 152*, 19–34. (h) Rathke, J. W.; Feder, H. M. *Ann. N.Y. Acad. Sci.* **1980**, *333*, 45–57. (i) Henrici-Olivé, G.; Olivé, S. *Angew. Chem., Int. Ed. Engl.* **1976**, *15*, 136–141. Henrici-Olivé, G.; Olivé, S. *J. Mol. Catal.* **1982**, 111–115. (j) Rofer-DePoorter, C. K. *Chem. Rev.* **1981**, *81*, 447–474. (k) Pichler, H.; Schulz, H. *Chem.-Ing.-Tech.* **1970**, *42*, 1162–1174.

(4) (a) Fagan, P. J.; Moloy, K. G.; Marks, T. J. *J. Am. Chem. Soc.* **1981**, *103*, 6959–6962. (b) Katahira, D. A.; Moloy, K. G.; Marks, T. J. *Organometallics* **1982**, *1*, 1723–1726. (c) Katahira, D. A.; Moloy, K. G.; Marks, T. J., manuscript in preparation.

(5) (a) Fagan, P. J.; Manriquez, J. M.; Marks, T. J. In "Organometallics of the f-Elements"; Marks, T. J., Fischer, R. D., Eds.; D. Reidel Publishing: Dordrecht, 1979; Chapter 4. (b) Marks, T. J.; Ernst, R. D. In "Comprehensive Organometallic Chemistry"; Wilkinson, G. W., Stone, F. G. A., Abel, E. W., Eds.; Pergamon Press: Oxford, 1982; Chapter 21. (c) Marks, T. J. *Science (Washington, D.C.)* **1982**, *217*, 989–997.

(6) Fagan, P. J.; Manriquez, J. M.; Marks, T. J.; Vollmer, S. H.; Day, C. S.; Day, V. W. *J. Am. Chem. Soc.* **1981**, *103*, 2206–2220.

(7) (a) Wayland, B. B.; Duttahmed, A.; Woods, B. A. *J. Chem. Soc., Chem. Commun.* **1983**, 143–143. (b) Wayland, B. B.; Woods, B. A.; Pierce, R. *J. Am. Chem. Soc.* **1982**, *104*, 302–303. (c) Wayland, B. B.; Woods, B. A. *J. Chem. Soc., Chem. Commun.* **1981**, 700–701.

(8) (a) Gladysz, J. A. *Adv. Organomet. Chem.* **1982**, *20*, 1–38 and references therein. (b) Tam, W. Lin, G.-Y.; Kiel, W. A.; Wong, V. K.; Gladysz, J. A. *J. Am. Chem. Soc.* **1982**, *104*, 141–152. (c) Steinmetz, G. R.; Geoffroy, G. L. *J. Am. Chem. Soc.* **1981**, *103*, 1278–1279. (d) Thorn, D. L. *Organometallics* **1982**, *1*, 197–204. (e) Casey, C. P.; Andrews, M. A.f McAlister, D. E.; Rinz, J. E. *J. Am. Chem. Soc.* **1980**, *102*, 1927–1933. (f) Wong, W.-K.; Tam, W.; Gladysz, J. A. *J. Am. Chem. Soc.* **1979**, *101*, 5440–5442. (g) Brown, K. L.; Clark, G. R.; Headford, C. E. L.; Marsden, K.; Roper, W. R. *J. Am. Chem. Soc.* **1979**, *101*, 503–505. (h) Collman, J. P.; Winter, S. R. *J. Am. Chem. Soc.* **1973**, *95*, 4089–4090. (i) Narayanan, B. A.; Amatore, C.; Casey, C. P.; Kochi, J. K. *J. Am. Chem. Soc.* **1983**, *105*, 6351–6352. (j) Summer, C. E.; Nelson, G. O. *J. Am. Chem. Soc.* **1984**, *106*, 432–433.

(9) (a) Wolczanski, P. T.; Threlkel, R. S.; Bercaw, J. E. *J. Am. Chem. Soc.* **1979**, *101*, 218–220. (b) Threlkel, R. S.; Bercaw, J. R. *J. Am. Chem. Soc.* **1981**, *103*, 2650–2659.

(10) (a) Belmonte, P. A.; Cloke, F. G. N.; Schrock, R. R. *J. Am. Chem. Soc.* **1983**, *105*, 2643–2650. (b) Churchill, M. R.; Wasserman, H. J. *Inorg. Chem.* **1982**, *21*, 226–230. (c) Belmonte, P.; Schrock, R. R.; Churchill, M. R.; Youngs, W. J. *J. Am. Chem. Soc.* **1979**, *101*, 2868–2860.

spectrometer. Chemical shifts are reported relative to internal Me_4Si. Infrared spectra were recorded on a Perkin-Elmer 599B spectrophotometer using either Nujol or Fluorolube mulls sandwiched between KBr plates in an o-ring sealed, air-tight holder. The apparatus and procedures for the determination of low-temperature infrared spectra have been described elsewhere.[12]

Elemental analyses and molecular weight determinations were performed by Dornis und Kolbe Mikroanalytisches Laboratorium, Mülheim, West Germany.

Materials and Methods. All operations were performed with rigorous exclusion of oxygen and moisture in Schlenk-type glassware on a dual manifold Schlenk line or interfaced to a high vacuum (10^{-5} torr) system or in a dinitrogen filled, Vacuum Atmospheres glovebox. Argon (Matheson, prepurified), carbon monoxide (Matheson, CP), dihydrogen (Linde), and deuterium gas (99.5%, Matheson) were purified by passage through a supported MnO oxygen removal column[13] and a Davison 4A molecular sieve column. ^{13}C-enriched carbon monoxide (90%, Stohler Isotopes) was used as received without further purification. All reaction solvents were distilled from Na/K/benzophenone under nitrogen and were condensed and stored in vacuo in bulbs on the vacuum line containing a small amount of $[Ti(\eta^5\text{-}C_5H_5)_2Cl]_2ZnCl_2$ as indicator.[14] Deuterated solvents were dried over Na/K alloy and vacuum transferred before use.

The complexes $Cp'_2Th(n\text{-}Bu)_2$,[15] $Cp'_2Th(CH_2\text{-}t\text{-}Bu)_2$,[16] Cp'_2ThMe_2,[16] Cp'_2ThCl_2,[16] and $Cp'_2ThCH_2C(CH_3)_2CH_2$[17] were prepared according to the literature procedures. The lithium reagents $LiCH_2\text{-}t\text{-}Bu$[18] and $LiCH_2SiMe_3$[19] were also prepared by known procedures. 2,6-Di-*tert*-butylphenol (Aldrich) was purified by sublimation or vacuum distillation. Di-*tert*-butyl ketone (Pfaltz and Bauer) was dried over molecular sieves and further purified by vacuum distillation. $t\text{-}Bu_2CHOH$ was prepared by $LiAlH_4$ reduction of $t\text{-}Bu_2CO$[20] and was vacuum sublimed before use.

Syntheses. $Cp'_2Th(Cl)(CH_2\text{-}t\text{-}Bu)$. In a modification of the procedure reported previously,[16] 5.50 g (9.69 mmol) of Cp'_2ThCl_2 and 0.83 g (10.6 mmol) of $LiCH_2\text{-}t\text{-}Bu_2$ were combined in a 100-mL flask. Heptane (65 mL) was added slowly via syringe while the flask and its contents were maintained at low temperature (liquid N_2 or dry ice). The colorless slurry was then stirred at −78 °C for ca. 1 h before the reaction was allowed to slowly warm to room temperature. After 2 h, the suspension was filtered, the colorless solid thus collected was washed with 15 mL of heptane, and the washings were combined with the mother liquor. The volume of heptane was then reduced in vacuo until a large amount of colorless crystals had formed, and the mixture was then cooled to −78 °C to crystallize more product. The resulting colorless, microcrystalline solid was isolated by filtration and was dried under high vacuum; ^1H NMR confirmed purity and identity: yield 4.46 g (7.73 mmol), 70%.

$Cp'_2Th(Me)(OCH\text{-}t\text{-}Bu_2)$, 1a. This complex was synthesized in a manner identical with that described for $Cp'_2Th(n\text{-}Bu)(OCH\text{-}t\text{-}Bu_2)$ (below) using 1.37 g (2.57 mmol) of Cp'_2ThMe_2 and 0.40 g (2.77 mmol) of $t\text{-}Bu_2CHOH$. The colorless, microcrystalline solid was isolated from cold (−78 °C) toluene and dried in vacuo: yield 1.28 g (1.94 mmol), 75%; NMR (C_6D_6) δ 3.67 (s, 1 H), 2.05 (s, 30 H), 1.07 (br s, 18 H), 0.40 (s, 3 H); IR (Nujol, cm^{-1}) 1395 (m), 1363 (m), 1264 (m), 1166 (w), 1104 (m), 105 (s), 1003 (s), 958 (m), 923 (w), 804 (m), 767 (m), 660 (s), 614 (w), 562 (w), 508 (m), 457 (w), 404 (m). Anal. Calcd for $C_{30}H_{52}OTh$: C, 54.53; H, 7.93. Found: C, 54.74; H, 7.94.

$Cp'_2Th(n\text{-}Bu)(OCH\text{-}t\text{-}Bu_2)$, 1b. $Cp'_2Th(n\text{-}Bu)_2$ (0.815 g, 1.32 mmol) was placed in a 50-mL two-neck flask fitted with a solid addition tube containing 0.20 g (1.39 mmol) of $t\text{-}Bu_2CHOH$. Toluene (15 mL) was added, and the resulting solution was cooled to −78 °C. The alcohol was then added to the solution, and the contents of the flask were warmed to room temperature to yield a clear, colorless solution. After 30 min of stirring, the solution was filtered and the toluene removed in vacuo to yield a waxy solid. After several heptane addition vacuum removal cycles the resulting colorless solid was dissolved in heptane and the solution was cooled to −78 °C overnight to yield a colorless microcrystalline solid which was isolated by cold filtration: yield 0.69 g (0.98 mmol), 74%; NMR (C_6D_6) δ 3.68 (s, 1 H), 2.02 (s, 30 H), 1.3–1.1 (m, 7 H), 1.05 (br s, 18 H), 0.63 (m, 2 H); IR (Nujol, cm^{-1}) 1392 (m), 1364 (m), 1048 (s), 998 (s), 957 (w), 769 (w), 722 (w), 656 (s). Anal. Calcd for $C_{33}H_{58}OTh$: C, 56.39; H, 8.32. Found: C, 56.08; H, 8.06.

$Cp'_2Th(Cl)(O\text{-}t\text{-}Bu)$. The following alternative route to this previously reported[16] complex was utilized for this work. Cp'_2ThCl_2 (3.00 g, 5.23 mmol) and 0.645 g (5.75 mmol) of freshly sublimed t-BuOK were combined in a 50-mL flask. After the flask was evacuated, 25–30 mL of Et_2O was condensed in at −78 °C and the apparatus backfilled with argon. The suspension was next warmed to room temperature and stirred for 3 h. At the end of this time, the Et_2O was removed in vacuo and replaced with 20 mL of toluene. The toluene was then filtered and removed in vacuo to yield a colorless, microcrystalline solid. The product was slurried into cold (−78 °C) pentane and isolated by filtration. ^1H NMR confirmed both identity and purity: yield 2.08 g (3.40 mmol), 65%.

$Cp'_2Th(CH_2\text{-}t\text{-}Bu)(O\text{-}t\text{-}Bu)$, 1c. $Cp'_2Th(Cl)(O\text{-}t\text{-}Bu)$ (2.025 g, 3.31 mmol) and 0.286 g (3.66 mmol) of $LiCH_2\text{-}t\text{-}Bu$ were combined in a 50-mL single-neck flask. After the vessel was evacuated, 25 mL of heptane was condensed in at −78 °C and the apparatus was placed under 1 atm of argon. After 10 min, the colorless suspension was allowed to warm to room temperature and stirring was continued for 2 h. At the end of this time, the insoluble LiCl was removed by filtration and the residue washed two times (Soxhlet extraction in vacuo) by condensing 3–4-mL portions of heptane from the filtrate into the upper portion of the filtration apparatus. These washings were combined with the filtrate, and the solvent was concentrated until a large amount of a colorless, crystalline solid began to precipitate, whereupon the contents of the flask were cooled to −78 °C. The product was isolated by filtration and dried in vacuo: yield 1.52 g (2.35 mmol), 71% NMR (C_6D_6) δ 2.04 (s, 30 H), 1.38 (s, 9 H), 1.31 (s, 9 H), 0.61 (s, 2 H); IR (Nujol, cm^{-1}) 1361 (s), 1263 (w), 1231 (s), 1206 (m), 1184 (s), 1102 (w), 1064 (w), 1021 (m), 990 (m), 963 (vs), 907 (w), 803 (w), 782 (s), 743 (m), 723 (w), 616 (w), 596 (w), 514 (s), 482 (s). Anal. Calcd for $C_{29}H_{50}OTh$: C, 53.86; H, 7.79. Found: C, 54.14; H, 7.88.

$Cp'_2Th(CH_2\text{-}t\text{-}Bu)(OCH\text{-}t\text{-}Bu_2)$, 1d. $Cp'_2Th(CH_2\text{-}t\text{-}Bu)_2$ (1.86 g, 2.87 mmol) was dissolved in 30 mL of cyclohexane. The resulting colorless solution was then placed in an oil bath at 60 °C until the conversion to the thoracyclobutane $Cp'_2Th[CH_2C(CH_3)_2CH_2]$ was complete. A sealed NMR tube containing the bis(alkyl) in C_6D_{12} or C_6D_6 was also placed in the oil bath so that the progress of the reaction could be monitored. After ca. 48 h, the conversion was judged to be complete and the reaction flask was removed from the oil bath. The now yellow-orange solution was filtered to remove a small amount of precipitate, and the solvent was removed in vacuo. NMR analysis of the resulting solid showed it to be 90–95% pure metallacycle. The solid was next suspended in 20 mL of heptane at −78 °C, and 0.47 g (3.26 mmol) of $t\text{-}Bu_2CHOH$ was added. The suspension was warmed to room temperature, whereupon much of the yellow-orange color faded and a colorless precipitate was observed. After 1 h, the volume of heptane was reduced by ca. half and the solution was cooled to −78 °C. The resulting solid was isolated by filtration, washed with cold heptane until the washings were colorless, and dried under vacuum: yield 1.25 g (1.74 mmol), 61%; NMR (C_6D_6) δ 3.78 (s, 1 H), 2.08 (s, 30 H), 1.40 (s, 9 H), 1.08 (s, 18 H); IR (Nujol, cm^{-1}) 1390 (m), 1386 (m), 1358 (m), 1347 (m), 1235 (m), 1203 (m), 1163 (w), 1110 (w), 1046 (s), 989 (s), 962 (w), 918 (w), 98 (w), 855 (w), 797 (w), 759 (w), 738 (w), 649 (s), 603 (w), 568 (w), 523 (w), 484 (w), 471 (w). Anal. Calcd for $C_{34}H_{60}OTh$: C, 56.97; H, 8.44. Found: C, 56.63; H, 8.58.

(11) Similarly, Lewis acid promotion of alkyl migratory CO insertion reactions has been observed as well as a stabilization of the resulting "acyls" via combined M–C and M′–O bonding: (a) Butts, S. B.; Strauss, S. H.; Holt, E. M.; Stimson, R. E.; Alcock, N. W.; Shriver, D. F. *J. Am. Chem. Soc.* **1980**, *102*, 5093–5100. (b) Richmond, T. G.; Basolo, F.; Shriver, D. F. *Inorg. Chem.* **1982**, *21*, 1272–1273. (c) Stimson, R. E.; Shriver, D. R. *Inorg. Chem.* **1980**, *19*, 1141–1145. (d) Butts, S. B.; Richmond, T. G.; Shriver, D. F. *Inorg. Chem.* **1981**, *20*, 278–280. (e) Grimmett, D. L.; Labinger, J. A.; Bonfiglio, J. N.; Masuo, S. T.; Shearin, E.; Miller, J. S. *Organometallics* **1983**, *2*, 1325–1332. (f) Labinger, J. A.; Bonfiglio, J. N.; Grimmett, D. L.; Masuo, S. T.; Shearin, E.; Miller, J. S. *Organometallics* **1983**, *2*, 733–740. (g) Labinger, J. A.; Miller, J. S. *J. Am. Chem. Soc.* **1982**, *104*, 6856–6858. (h) Grimmett, D. L.; Labinger, J. A.; Bonfiglio, J. N.; Masuo, S. T.; Shearin, E.; Miller, J. S. *J. Am. Chem. Soc.* **1982**, *104*, 6858–6859. (i) Collman, J. P.; Finke, R. G.; Cawse, J. N.; Brauman, J. I. *J. Am. Chem. Soc.* **1978**, *100*, 4766–4772.

(12) (a) Marks, T. J. *J. Chem. Educ.* **1971**, *48*, 167. (b) Sonnenberger, D. C.; Mintz, E. A.; Marks, T. J. *J. Am. Chem. Soc.*, in press.

(13) McIlwrick, C. R.; Phillips, C. S. G. *J. Chem. Phys. E* **1973**, *6*, 1208–1210.

(14) Sekutowski, D. G.; Stucky, G. D. *J. Chem. Educ.* **1976**, *53*, 110.

(15) (a) Bruno, J. W.; Marks, T. J.; Morss, L. R. *J. Am. Chem. Soc.* **1983**, *105*, 6824–6832. (b) Sonnenberger, D. C.; Marks, T. J.; Morss, L. R., *Organometallics*, in press. (c) Bruno, J. W.; Duttera, M. R.; Fendrick, C. M.; Smith, G. M.; Marks, T. J. *Inorg. Chim. Acta* **1984**, *94*, 271–277. (d) Sonnenberger, D. C.; Marks, T. J., submitted for publication.

(16) Fagan, P. J.; Manriquez, J. M.; Maatta, E. A.; Seyam, A. M.; Marks, T. J. *J. Am. Chem. Soc.* **1981**, *103*, 6650–6667.

(17) (a) Bruno, J. W.; Marks, T. J.; Day, V. W. *J. Organomet. Chem.* **1983**, *250*, 237–246. (b) Bruno, J. W.; Marks, T. J.; Day, V. W. *J. Am. Chem. Soc.* **1982**, *104*, 7357–7360.

(18) Collier, M. R.; Lappert, M. F.; Pearce, R. *J. Chem. Soc., Dalton Trans.* **1973**, 445–451.

(19) Schrock, R. R.; Fellman, J. D. *J. Am. Chem. Soc.* **1978**, *100*, 3359–3370.

(20) Nystrom, R. F.; Brown, W. G. *J. Am. Chem. Soc.* **1947**, *69*, 1197–1199.

$[Cp'_2Th(\mu\text{-}H)(H)]_2$. The following is a one-pot synthesis of the previously reported[16] title complex starting from Cp'_2ThCl_2. Cp'_2ThCl_2 (5.00 g, 8.72 mmol) and 1.70 g (18.1 mmol) of $LiCH_2SiMe_3$ were placed in a 100-mL flask. After the flask was evacuated, 35 mL of Et_2O was condensed into the flask at −78 °C and the vessel was then backfilled with argon (1 atm). After 20–30 min, the slurry was allowed to warm to room temperature and stirring was continued for 3 h. The Et_2O was then removed under vacuum and replaced with 35 mL of heptane. The solution was filtered, and the residual solids were washed by condensing some of the heptane from the filtrate into the upper portion of the filtration apparatus. The colorless solution was then degassed and placed under 1 atm of H_2 with vigorous stirring. Within 5 min, the colorless solution turned bright yellow, and after 0.5 h, large amounts of a pale yellow solid had formed. After 6 h, a fresh charge of H_2 (1 atm) was admitted to the flask and stirring was continued overnight. The solid was isolated by filtration, washed with 5 mL of heptane, and dried in vacuo: ^1H NMR confirmed both identity and purity; yield 3.80 g (3.77 mmol), 86%. $[Cp'_2Th(\mu\text{-}D)(D)]_2$ was prepared in a like manner using D_2.

$Cp'_2Th(H)(OCH\text{-}t\text{-}Bu_2)$, 1e. $[Cp'_2Th(H)(\mu\text{-}H)]_2$ (1.00 g, 0.991 mmol) and a magnetic stir bar were placed in a 50-mL one-neck flask fitted with a 9-mm Fischer-Porter Solv-Seal joint. Toluene (25 mL) was added, followed by 0.40 mL (0.33 g, 2.33 mmol) of $t\text{-}Bu_2CO$. The flask was fitted with a Teflon vacuum valve, and the apparatus was attached to the vacuum line where the yellow solution was degassed (to remove N_2) and placed under an argon atmosphere. The reaction vessel was then immersed in an 80 °C oil bath such that the oil level was coincident with the solution level. After 75 min, the solution had turned from yellow to colorless, and the flask was removed from the oil bath. The solution was next filtered, and the volume of toluene filtrate was reduced to ca. 5 mL. Next, 5–10 mL of heptane was added and the contents of the flask were slowly cooled to −78 °C. The resulting colorless crystals were isolated by cold filtration and dried in vacuo: yield 0.90 g (1.4 mmol), 71%; NMR (toluene-d_8) δ 17.1 (s, 1 H), 3.50 (s, 1 H), 2.23 (s, 30 H), 1.18 (br s, 18 H); IR (Nujol, cm^{-1}) 2492 (m), 1355 (s), 1164 (w), 1053 (s), 1030 (w), 1003 (s), 960 (w), 924 (w), 801 (w), 768 (w), 722 (w), 663 (s). Anal. Calcd for $C_{29}H_{50}OTh$: C, 53.85; H, 7.79; M_r, 647 g/mol. Found: C, 54.10; H, 7.66; M_r, 760 g/mol (cryoscopic in benzene). Upon prolonged exposure to fluorescent lighting, this complex develops a purple color and therefore should be stored in the dark.

$Cp'_2Th(D)(OCH\text{-}t\text{-}Bu_2)$, 1e-Th$_d$. $Cp'_2Th(H)(OCH\text{-}t\text{-}Bu_2)$ (0.36 g, 0.57 mmol) was placed in a 25-mL one-neck flask fitted with a 9-mm Fischer-Porter Solv-Seal joint and a Teflon stopcock. After the flask was evacuated 10 mL of toluene was condensed into the flask and it was next backfilled with 1 atm of D_2. The flask was immersed in a 110 °C oil bath for 8 h before the colorless solution was degassed and a fresh charge of D_2 was added. After this procedure was repeated one more time, the solution was cooled to room temperature and the toluene was removed under vacuum to yield a colorless powder. If necessary, this material may be recrystallized from toluene/heptane in a manner identical with that used for $Cp'_2Th(H)(OCH\text{-}t\text{-}Bu_2)$ (vide supra): NMR (C_6D_6) δ 3.50 (s, 1 H), 2.23 (s, 30 H), 1.18 (s, 18 H); IR (Nujol, cm^{-1}) $\nu_{Th\text{-}D}$ 971 (s).

$Cp'_2Th(H)(OCD\text{-}t\text{-}Bu_2)$, 1e-C$_d$. $[Cp'_2Th(D)(\mu\text{-}D)]_2$ (0.250 g, 0.247 mmol) and 0.095 mL (0.079 g, 0.55 mmol) of $t\text{-}Bu_2CO$ were reacted in 7 mL of toluene in the same manner as that used to synthesize $Cp'_2Th(H)(OCH\text{-}t\text{-}Bu_2)$ above. After 1.5 h at 80 °C, the toluene was removed under vacuum, and the resulting colorless solid was analyzed by NMR. The ^1H NMR spectra exhibited resonances attributable to the $\eta^5\text{-}C_5(CH_3)_5$ and t-Bu protons of $Cp'_2Th(D)(OCD\text{-}t\text{-}Bu_2)$ at δ 2.23 an 1.18, respectively; resonances attributable to hydride (17.1 ppm) and methine (3.50 ppm) protons were completely absent, consistent with >98% deuteration. The solid was redissolved in 10 mL of heptane and placed under 1 atm of H_2. The solution was then heated to 110 °C for 8 h after which time the solution was degassed and placed under a fresh charge of H_2. After the solution was heated (110 °C) for 8 h longer, this procedure was repeated one more time to give a total of three H_2 purges and a reaction time of 24 h. The solution was then filtered and the solvent removed under vacuum until colorless crystals began to precipitate. After the solution was cooled slowly to −78 °C, the complex was isolated by cold filtration and dried in vacuo: yield 0.155 g (2.39 mmol), 48%; NMR (C_6D_6) δ 17.1 (s, 1 H), 2.23 (s, 30 H), 1.18 (s, 18 H); IR (Nujol, cm^{-1}) ν_{CD} 2100 (w).

$Cp'_2Th(H)(2,6\text{-}t\text{-}Bu_2C_6H_3O)$, 1f. $[Cp'_2Th(H)(\mu\text{-}H)]_2$ (1.00 g, 0.991 mmol) and 0.42 g (2.02 mmol) of $2,6\text{-}t\text{-}Bu_2C_6H_3OH$ were placed in a 50-mL one-neck flask fitted with a Fischer-Porter Solv-Seal joint and a Teflon stopcock. The apparatus was evacuated, 20–25 mL of toluene was condensed in, and the flask was backfilled with 0.8 atm of argon. The vessel next was immersed in a 60 °C oil bath such that the oil level was coincident with the solution level. After 12 h the initially yellow solution was almost colorless and was allowed to cool to room temperature. The solution was then filtered and the solvent volume reduced until only ca. 2 mL of toluene remained, yielding a colorless precipitate. Then, 5–10 mL of heptane was added and the slurry was gently warmed to dissolve the product. Allowing the solution to slowly cool to −78 °C resulted in the formation of colorless crystals that were isolated by filtration and dried under vacuum: yield 1.21 g (1.71 mmol), 86%; NMR (C_6D_6) δ 19.1 (s, 1 H), 7.0 (m, 3 H), 2.03 (s, 30 H), 1.52 (s, 18 H); IR (Nujol, cm^{-1}) 1407 (s), 1365 (m), 1261 (w), 1223 (s), 1200 (m), 1122 (m), 1096 (w), 1020 (w), 865 (s), 823 (m), 794 (w), 748 (m), 660 (m). Anal. Calcd for $C_{34}H_{52}OTh$: C, 57.61; H, 7.39; M_r, 709 g/mol. Found: C, 57.60; H, 7.45; M_r, 822 g/mol (cryoscopic in benzene). Upon prolonged exposure to fluorescent lighting this complex develops a purple color and therefore should be stored in the dark.

$Cp'_2Th(\eta^2\text{-}COMe)(OCH\text{-}t\text{-}Bu_2)$, 5a. Carbonylation of complex **1a** was carried out under 780 torr of CO at 0 °C in toluene solution. After 24 h at 0 °C, solvent and CO were removed from the yellow solution in vacuo to yield a pale yellow powder. NMR analysis of the resulting material showed that the reaction was only ca. 40% complete. Longer reaction times and higher temperatures gave increasing amounts of secondary reaction products and a further color change from yellow to deep purple: NMR (C_6D_6) δ 3.65 (s, 1 H), 2.60 (s, 3 H), 1.99 (s, 30 H), 1.19 (s, 9 H).

The complex $Cp'_2Th(\eta^2\text{-}^{13}COMe)(OCH\text{-}t\text{-}Bu_2)$ (**5a***) was generated in a similar fashion using ^{13}CO: $^{13}C\{^1H\}$ NMR (C_6D_6) 362 ppm.

$Cp'_2Th(\eta^2\text{-}CO\text{-}n\text{-}Bu)(OCH\text{-}t\text{-}Bu_2)$, 5b. Complex **1b** (0.50 g, 0.71 mmol) was placed in a 25-mL flask containing a magnetic stir bar. After the flask was evacuated 5–10 mL of toluene was condensed in at −78 °C. The colorless solution was then warmed to −5 °C with an ice bath, and the apparatus was backfilled with 0.8 atm of CO, whereupon the solution rapidly developed a yellow color. After 1 h of stirring, the solution was warmed to room temperature and filtered and solvent removed in vacuo to yield a dull yellow powder. The powder was slurried into 2 mL of heptane at −78 °C and filtered while cold: yield 0.37 g (5.1 mmol), 71%; NMR (C_6D_6) δ 3.87 (s, 1 H), 3.10 (m, 2 H), 2.06 (s, 30 H), 1.9–0.7 (m, 7 H), 1.22 (br s, 18 H); IR (Nujol, cm^{-1}) 1388 (m), 1363 (m), 1324 (w), 1235 (w), 1216 (w), 1165 (w), 1111 (w), 1055 (s), 1037 (w), 1028 (w), 1001 (s), 959 (m), 921 (w), 861 (w), 806 (w), 769 (m), 722 (w), 651 (s), 617 (w), 599 (w), 563 (w), 527 (w); (Fluorolube) 1479 (s). Anal. Calcd for $C_{34}H_{58}O_2Th$: C, 55.88; H, 8.00. Found: C, 55.97; H, 7.89.

The complex $Cp'_2Th(\eta^2\text{-}^{13}CO\text{-}n\text{-}Bu)(OCH\text{-}t\text{-}Bu_2)$ (**5b***) was prepared from **1b** and ^{13}CO: $^{13}C\{^1H\}$ NMR (C_6D_6) δ 356; IR (Fluorolube) 1447 cm^{-1}.

$Cp'_2Th(\eta^2\text{-}COCH_2\text{-}t\text{-}Bu)(O\text{-}t\text{-}Bu)$, 5c. $Cp'_2Th(CH_2\text{-}t\text{-}Bu)(O\text{-}t\text{-}Bu)$ (0.82 g, 1.27 mmol) was placed in a 25-mL flask that was subsequently evacuated. Next, 10 mL of toluene was condensed in at −55 °C, and the flask was backfilled with 650 mm of CO, with vigorous stirring. The initially clear, colorless solution rapidly turned yellow, and gas uptake was noted. After 1.5 h, CO and solvent were removed in vacuo to yield a gummy foam that defied all attempts to crystallize. NMR analysis shows that the material thus obtained is approximately 90–95% pure: NMR (C_6D_6) δ 2.69 (s, 2 H), 2.03 (s, 30 H), 1.39 (s, 9 H), 1.21 (s, 9 H); IR (Nujol, cm^{-1}) 1369 (s), 1320 (w), 1228 (m), 1186 (s), 1125 (w), 1089 (w), 1022 (m), 964 (vs), 805 (w), 777 (s), 724 (w), 616 (m), 595 (m), 561 (m), 483 (m); (Fluorolube) 1472 cm^{-1}.

The complex $Cp'_2Th(\eta^2\text{-}^{13}COCH_2\text{-}t\text{-}Bu)(O\text{-}t\text{-}Bu)$ (**5c***) was prepared similarly with ^{13}CO: $^{13}C\{^1H\}$ NMR (C_6D_6) δ 362; IR (Fluorolube) ca. 1443 cm^{-1}.

$Cp'_2Th(\eta^2\text{-}COCH_2\text{-}t\text{-}Bu_2)(OCH\text{-}t\text{-}Bu_2)$, 5d. $Cp'_2Th(CH_2\text{-}t\text{-}Bu)(OCH\text{-}t\text{-}Bu_2)$ (0.60 g, 0.84 mmol) was suspended in 15 mL of heptane at −78 °C. The solution was then placed under 1 atm of CO, whereupon the solution began to gradually take on a yellow color. The solution was next warmed to 0 °C, and after 5–10 min, all of the solid starting material had dissolved to yield a bright yellow solution. After 0.5 h, the CO was pumped off and the solution was filtered. The heptane was then removed under vacuum until a bright yellow crystalline solid began to precipitate, whereupon the solution was cooled to −78 °C. The resulting solid was isolated by cold filtration and dried in vacuo: yield 0.27 g. An additional 0.15 g of product was isolated from the mother liquor to give a total yield 0.42 g (0.56 mmol) (67%): NMR (C_6D_6) δ 3.86 (s, 1 H), 3.26 (s, 2 H), 2.02 (s, 30 H), 1.19 (br s, 18 H), 1.15 (s, 9 H); IR (Nujol, cm^{-1}) 1387 (m), 1354 (s), 1307 (m), 1273 (w), 1249 (m), 1215 (w), 1162 (w), 1110 (w), 1055 (s), 1037 (w), 1003 (s), 957 (m), 931 (w), 920 (w), 885 (w), 858 (w), 800 (w), 765 (m), 718 (w), 647 (s), 610 (w), 571 (w), 530 (w); (Fluorolube) 1453 cm^{-1}. Anal. Calcd for $C_{35}H_{69}O_2Th$: C, 56.44; H, 8.12. Found: C, 56.44; H, 8.60.

$Cp'_2Th(\eta^2\text{-}^{13}COCH_2\text{-}t\text{-}Bu)(OCH\text{-}t\text{-}Bu_2)$ (**5d***), was prepared in a similar manner using ^{13}CO: $^{13}C\{^1H\}$ NMR (C_6D_6) δ 359.5; IR (Fluorolube, cm^{-1}) 1434.

Spectroscopic Characterization of Formyl Complexes 8a and 8b. In a typical experiment, 30 mg of the appropriate hydride complex (**1e** or **1f**) was placed in a 5-mm NMR tube that was then attached to a vacuum

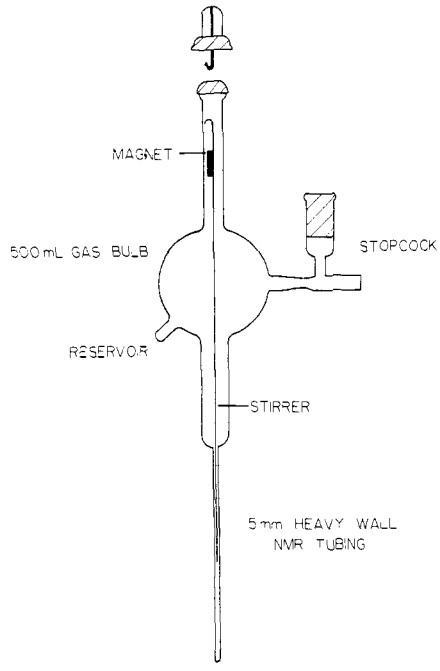

Figure 1. Schematic of the gas bulb/NMR tube used for equilibrium and kinetic studies.

line adaptor/stopcock. After the tube was evacuated, 0.5 mL of toluene-d_8 was condensed in at −78 °C. finally, the desired pressure of ^{12}CO or ^{13}CO (0.5–1.5 atm) was admitted and the tube sealed with a torch.

Complex **8a**: ^1H NMR δ 1.07 (br s, 18 H), 2.17 (br s, 30 H), 3.70 (2, 1 H), 15.2 (s, 1 H); ^{13}C NMR (**8a***): 372 ppm ($^1J_{^{13}C-H}$ = 114 Hz).

Complex **8b**: ^1H NMR δ 1.65 (br s, 18 H), 1.93 (s, 30 H), 7.0 (m, 3 H), 14.71 (s, 1 H); ^{13}C NMR (**8b***) 360 ppm ($^1J_{^{13}C-H}$ = 117 Hz).

Low-temperature (<−50 °C) infrared spectra were measured in THF or THF-d_8 solution in a manner described previously.[12] For complex **8a**, ν_{CO} = 1447 cm^{-1} and, for **8a***, $\nu_{^{13}CO}$ = 1443 cm^{-1}.

Thermodynamic Studies of Hydride Carbonylation. In order to quantify the temperature dependent formyl equilibrium, the apparatus shown in Figure 1 was employed. The large (500 mL) gas bulb attached to the NMR tube ensured a known, constant pressure of CO above the NMR solution. Carbon monoxide solubilities were taken from the literature.[21] In a typical experiment, 35 mg (5.4 × 10^{-2} mmol) of **1e** was dissolved in 0.60 mL of toluene-d_8 and the resulting colorless solution was transferred to the reservoir of the gas bulb/NMR tube in the glovebox. The apparatus was attached to the vacuum line, and the solution was then freeze–pump–thaw degassed three times. The bulb was then tilted such that the solution flowed into the NMR tube portion of the apparatus and the solution was cooled to −78 °C. Next, the system was charged with the desired pressure of CO using a mercury U-tube manometer. The stopcock leading to the apparatus was then closed, and the NMR tube was inserted into the probe of a JEOL FX-90Q NMR spectrometer. The instrument had been previously tuned to maximize field homogeneity under nonspinning conditions and the probe cooled to low temperature (−80 °C). The "stirrer" (a stainless steel or quartz rod attached to a magnet) was then lifted from its holder with the aid of an external magnet, and the solution was agitated for several minutes to ensure equilibration with the CO atmosphere. The stirrer was then placed back onto the holder, and the NMR spectrum was recorded in the usual manner. Before the ^1H NMR spectrum was recorded at a different temperature, the solution was agitated for several minutes in order for the CO concentration to reach equilibrium. Equilibrium constants were measured by integration of the well-resolved formyl CHO (ca. 15 ppm) and hydride ThH (ca. 18 ppm) resonances. Sufficiently long pulse delays were employed to ensure accurate integration.

Determination of K_H/K_D and k_H/k_D for the Equilibrium 1e + CO ⇌ 8a. In the glovebox, 20 mg (3.1 × 10^{-2} mmol) each of complexes **1e-Th$_d$** and **1e-C$_d$** were placed in a locally modified[22] version of a Wilmad 524 PP NMR tube (5 mm) fitted with a Fischer-Porter pressure valve. The tube was next closed, connected to a vacuum line adaptor, and removed from the glovebox. After the device was attached to the vacuum line, the contents were evacuated and 0.50 mL of toluene-d_8 was condensed in at −78 °C. A pressure of 400 torr of CO was next introduced into the tube, the stopcock was closed, and the tube was disconnected from the adaptor. The sample was then placed in the probe of a JEOL FX-270 spectrometer that had been previously cooled to −78.5 ± 0.5 °C. The ^1H NMR spectrum was then recorded at this temperature. Integration of the Th–H resonance of **1e-C$_d$** and the ThCHO resonance of **8a-C$_d$** vs. the alkoxide methine protons of complexes **1e-Th$_d$** and **8a-Th$_d$** provided a measure of K_H/K_D. Also, the line widths were measured at this temperature in order to determine the natural line widths in the stopped exchange region. The probe was then warmed to −58 °C, whereupon

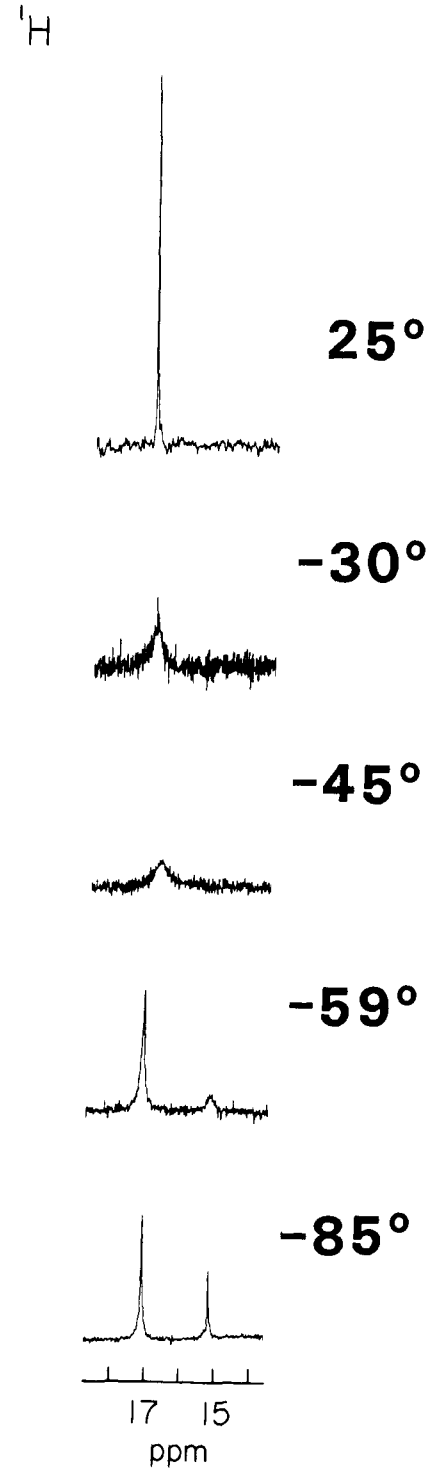

Figure 2. Variable-temperature FT 90-MHz ^1H NMR spectra of **1e** as a 0.077 M toluene-d_8 solution in the presence of 530 torr of CO. The resonances at 17.2 and 15.2 ppm are attributed to **1e** and **8a**, respectively.

(21) (a) Gjaldbaek, J. C.; Andersen, E. K. *Acta Chem. Scand.* **1954**, *8*, 1398–1413. (b) Seidell, A.; Linke, W. F. "Solubilities of Inorganic and Metal Organic Compounds", 4th ed.; Van Nostrand: New York, 1958; Vol. 1.

(22) Suzuki, H.; Marks, T. J., unpublished results. The device is a modified version of that sold commercially (Wilmad Glass Co., Inc., catalog number 528-PP, pressure valve NMR tube).

broadening of exchanging resonances was observed to occur (refer to Figure 2). The spectrum was recorded, and the line widths were measured in this slow-exchange region. The rate of chemical exchange in this region is simply the difference in line widths between slow and stopped exchange.[23] The line widths of resonances not involved in the site-exchange process were invariant between −78.5 and −58 °C.

$Cp'_2Th(n\text{-Bu})(OCH\text{-}t\text{-}Bu_2)$ + CO Reaction Kinetics. In a typical measurement, 0.150 g of **1b** was placed in a reaction bulb containing a stir bar and a Kontes valve-to-vacuum line adaptor. Toluene (10 mL) was added, and the apparatus was removed from the glovebox. It was then attached to a high vacuum line. The solution was freeze–pump–thaw degassed three times and then immersed with stirring in a low-temperature bath held at −54 ± 0.2 °C with a NESLAB CC-80II immersion cooler. Once the temperature had stabilized, the apparatus was backfilled with the desired pressure of CO. Pressure measurements were accomplished with a cathetometer and a U-tube manometer.[24] Recordings were begun ca. 2 min after the start of the reaction to allow equilibration. The total change in CO pressure was kept at ≤5% in order to approach pseudo-first-order conditions (using various portions of the vacuum line as ballast).

Carbonylation reactions were monitored for 3 half-lives. Plots of $\ln (P_0 - P_\infty / P - P_\infty)$ vs. time and k_{obsd} vs. P_{CO} were fit by standard linear regression techniques to obtain the second-order rate constant.

Determination of Reaction Orders for Thorium Hydride Carbonylation by NMR. Complex **1e** (0.2098 g, 0.3244 mmol) was placed in a 5-mL volumetric flask which was then filled with toluene-d_8 in the glovebox to give a 6.49×10^{-2} M stock solution of hydride. A 0.50-mL aliquot was placed in the gas bulb/NMR tube apparatus described above. After the solution was degassed, the bulb was backfilled with 878 torr of CO while the solution was kept at −78 °C. After the solution had equilibrated with CO at this temperature, the apparatus was placed in the probe of a JEOL FX-90Q spectrometer that had been previously tuned to maximize field homogeneity under nonspinning conditions and the probe cooled to −83 °C. The solution was again stirred to ensure CO equilibration, the stirrer was placed in its holder, and the spectrum was recorded in the usual manner. The line widths of hydride and formyl resonances in this stopped exchange region (see Figure 6) were determined to be 12–13 Hz, due to the nonspinning conditions employed. The sample was then warmed to −54 °C, the solution was stirred for several minutes, and the NMR spectrum was again recorded. The formyl CHO line width in this slow to intermediate exchange region was determined to be 32 Hz, corresponding to a 19 ± 3 Hz line broadening due to site exchange. The line widths of peaks not involved in site exchange were invariant between −83 and −54 °C.

Next, a 1.0-mL aliquot of the stock solution of **1e** was quantitatively diluted to 5.0 mL with toluene-d_8, yielding a 1.30×10^{-2} M solution. A 0.50-mL aliquot of this solution was placed in the gas bulb/NMR tube, and after it was degassed, etc. in the usual way, 878 torr of CO was admitted to the device. The low-temperature ^1H NMR spectra were recorded as described above. At −54 °C, the line broadening due to exchange was found to be 16 ± 3 Hz. These spectra are shown in Figure 6. During the course of these experiments, care was taken in field homogeneity adjustments to ensure that the line widths of nonexchanging resonances (i.e., aromatic solvent protons) did not vary by more than 1–2 Hz.

Crossover Experiment between $1e\text{-}Th_d$ and 1f in the Presence of CO. Complexes **1f** (25 mg, 3.5×10^{-2} mmol) and $1e\text{-}Th_d$ (23 mg, 3.6×10^{-2} mmol) were placed in a 5-mm NMR tube that was then attached to a vacuum line adaptor/stopcock via a vacuum-tight Teflon connector. After the tube was evacuated, ca. 0.5 mL of toluene-d_8 was condensed into the tube and the complexes were dissolved at −78 °C to yield a colorless solution. The tube was backfilled with ca. 1 atm of CO, the stopcock closed, and the tube immersed in liquid nitrogen. The tube was then sealed with a torch and the frozen solution allowed to thaw at −78 °C, yielding a bright yellow solution. The tube was placed in the probe of a JEOL FX-90Q spectrometer that had been previously cooled to −80 °C. ^1H NMR spectra showed the presence of **1f** (19.1 ppm) and **8b** (14.7 ppm) (see Figure 3) only. After 1 h at this temperature, the ^1H NMR showed that no detectable (i.e., <5%) scrambling of hydrogen and deuterium had occurred.

$Cp'_2Th(R)(OR')$ + CO Insertion Kinetics. Estimation of Second-Order Rate Constants. Method a. In a typical experiment, 30 mg of $Cp'_2Th(CH_2\text{-}t\text{-}Bu)(OCH\text{-}t\text{-}Bu_2)$ dissolved in 0.50 mL of toluene-d_8 was placed in a 25-mL flask fitted with a Kontes valve-to-vacuum line adaptor. The solution was freeze–pump–thaw degassed and then placed in a thermostated bath at −54 ± 0.2 °C. The flask was next backfilled with 257 torr of CO (a large volume of CO ensured a negligible change in CO pressure during the measurement, i.e., pseudo-first-order conditions), and the reaction was allowed to proceed, with vigorous stirring, for exactly 5.0 min before the CO was removed under vacuum. The solution (now slightly yellow) was then transferred to an NMR tube for ^1H analysis. The extent of the reaction was determined by measurement of the peak areas of both the methine and methylene resonances in starting material and product by the cut and weigh method. The reaction was assumed to obey second-order kinetics and an approximate rate constant was calculated via eq 7. This method was also applied to $Cp'_2Th(Me)(OCH\text{-}t\text{-}Bu_2)$.

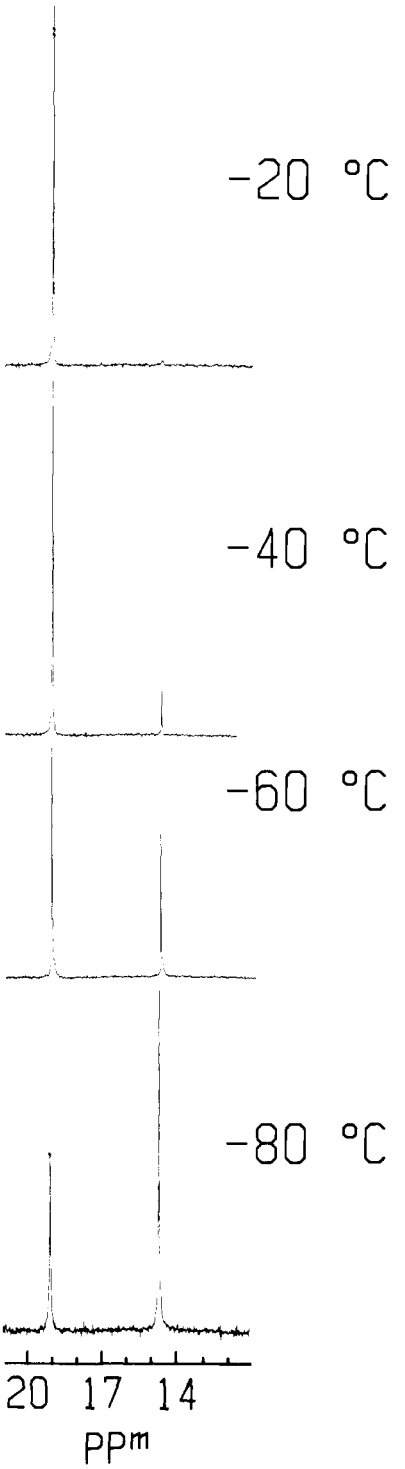

Figure 3. Variable-temperature FT 90-MHz ^1H NMR spectra of **1f** as a 0.09 M toluene-d_8 solution in the presence of 1.5 atm of CO. The resonances at 19.1 and 14.7 ppm are attributed to **1f** and **8b**, respectively.

(23) (a) Becker, E. "High Resolution NMR. Theory and Applications"; Academic Press: New York, 1980; Chapt. 11. (b) Binsch, G. In "Dynamic Nuclear Magnetic Resonance Spectroscopy"; Jackman, L. M., Cotton, F. A., Eds.: Academic Press: New York, 1976; pp 47–51.

(24) Shriver, D. F. "The Manipulation of Air-Sensitive Compounds"; McGraw-Hill: New York, 1969.

$$k = 1/P_{CO}t \ln [A]_0/[A]_t \quad (7)$$

Method b. When the difference in k between two complexes was determined to be an order of magnitude or less (i.e., **5c** vs. **5d**) or if the carbonylation was very rapid at −54 °C (i.e., $Cp'_2Th(Cl)(CH_2\text{-}t\text{-}Bu)$), the rate constants were estimated by competition experiments. In a typical experiment, 30 mg (4.6×10^{-2} mmol) of **5c** and 33 mg (4.6×10^{-2} mmol) of **5d** were dissolved in 1 mL of toluene-d_8 and placed in a 25-mL flask along with a stir bar. The flask was attached to a calibrated gas addition bulb, which was then attached to the vacuum line. The solution was freeze–pump–thaw degassed three times. The stopcock leading to the flask was then closed, and a pressure of 25 torr of CO was introduced (bulb volume = 33.9 mL; bulb temperature = 296 K) to provide 4.6×10^{-2} mmol of CO. The stopcock leading to the vacuum line was closed, and the CO was admitted to the solution with rapid stirring. After 1 h at −54 °C, the solution was warmed to room temperature, transferred to an NMR tube, and analyzed. The quantity of each alkyl remaining was determined by the cut and weigh method using the ^1H methylene resonances for each alkyl and acyl complex. The ratio of the rate constants was determined via eq 8. Since the rate constant for carbonylation of **5d** was determined by method a, the rate constant for carbonylation of **5c** could be readily calculated.

$$k_A/k_B = \frac{\ln ([A]_0/[A]_t)}{\ln ([B]_0/[B]_t)} \quad (8)$$

The rate constant for the carbonylation of $Cp'_2Th(Cl)(CH_2\text{-}t\text{-}Bu)$ was determined in an identical manner using **5c** as the competing alkyl.

Results

Synthesis and Properties of Precursor Alkyls and Hydrides. The thorium alkyls and hydrides utilized in this study were prepared via the routes shown in eq 9–15. The synthetic methodologies

$$Cp'_2ThR_2 + R'OH \rightarrow Cp'_2Th(R)(OR') \quad (9)$$
1a, R = Me, R′ = CH-*t*-Bu$_2$
1b, R = *n*-Bu, R′ = CH-*t*-Bu$_2$

$$Cp'_2Th(Cl)(OR') + LiR \rightarrow Cp'_2Th(R)(OR') + LiCl \quad (10)$$
1c, R = CH_2-*t*-Bu, R′ = *t*-Bu

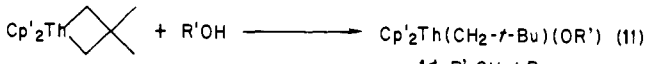

$$[Cp'_2Th(\mu\text{-}H)(H)]_2 + 2t\text{-}Bu_2CO \rightarrow Cp'_2Th(H)(OCH\text{-}t\text{-}Bu_2)$$
1e (12)

$$[Cp'_2Th(\mu\text{-}D)(D)]_2 + t\text{-}Bu_2CO \rightarrow Cp'_2Th(D)(OCD\text{-}t\text{-}Bu_2)$$
$$\xrightarrow{H_2} Cp'_2Th(H)(OCD\text{-}t\text{-}Bu_2) + HD \quad (13)$$
1e-C$_d$

$$Cp'_2Th(H)(OCH\text{-}t\text{-}Bu_2) + D_2 \rightarrow$$
$$Cp'_2Th(D)(OCH\text{-}t\text{-}Bu_2) + HD \quad (14)$$
1e-Th$_d$

$$[Cp'_2Th(\mu\text{-}H)(H)]_2 + 2,6\text{-}t\text{-}Bu_2C_6H_3OH \rightarrow$$
$$Cp'_2Th(H)(OC_6H_3\text{-}2,6\text{-}t\text{-}Bu_2) + 2H_2 \quad (15)$$
1f

presented here involve alcoholysis of actinide alkyls, metathesis of actinide halides with lithium reagents, ketone insertion into actinide hydride bonds, and deuterium/hydrogen exchange with actinide hydrides/deuterides. These types of reactions have been amply exploited and discussed in previous studies[16,25] and will not be dealt with in further detail here. The outcome of each of the above reactions is, however, critically dependent upon the particular choice of alkyl and alkoxide. For instance, addition of *t*-Bu$_2$CHOH (1 equiv) to Cp'_2ThMe_2 proceeds cleanly to yield **1a** while the same reaction with $Cp'_2Th(CH_2\text{-}t\text{-}Bu)_2$ (**2**) produces a mixture of **1d**, $Cp'_2Th(OCH\text{-}t\text{-}Bu_2)_2$ (**3**), and **2**. Also, the addition of 2 equiv of *t*-Bu$_2$CHOH to $[Cp'_2Th(\mu\text{-}H)(H)]_2$ (**4**) results in the formation of a 1:1 mixture of **3** and unreacted **4**. Conversely, the reaction of **4** with 2 equiv of 2,6-*t*-Bu$_2$C$_6$H$_3$OH produces complex **1f** in high yields. The syntheses reported herein are therefore specific for a given choice of hydrocarbyl/alkoxide and are often not interchangeable. The reasons for these observations are not clearly understood at the present time, but this phenomenon has been noted before.[25]

These new complexes displayed expected spectral (^1H NMR, IR) and analytical properties (see Experimental Section for details). In particular, the hydrides exhibit very low-field ^1H chemical shifts (17–19 ppm) and may be compared with those observed for $[Cp'_2Th(H)(\mu\text{-}H)]_2$ (19.2 ppm), $[Cp'_2Th(Cl)(\mu\text{-}H)]_2$ (19.0 ppm), and $Cp'_2Th(H)(O\text{-}t\text{-}Bu)$ (17.4 ppm).[16,25] Also, the terminal Th–H stretching vibrations at 1355 (**1e**) and 1365 cm^{-1} (**1f**) compare favorably with those reported previously (ca. 1350 cm^{-1}).[16,25] Deuterium substitution for hydride in complex **1e** results in a value for $\nu_{Th\text{-}D}$ of 971 cm^{-1}, a shift very close to that predicted by a Hooke's law calculation ($\nu_{Th\text{-}H}/\nu_{Th\text{-}D} = 1.40$).

The steric bulk of the −OCH-*t*-Bu$_2$ and −OC$_6$H$_3$-2,6-*t*-Bu$_2$ ligands employed in this study was found to be sufficient to result in hindered rotation of these alkoxide groups. Thus, the hydride complexes exhibit magnetically nonequivalent Cp′ (**1e**) and *t*-Bu resonances (**1e**,**1f**) at 0 °C and 90 MHz (or 25 °C and 270 MHz). These observations are readily understood in terms of the Newman projections shown below. In each of these views, it is assumed

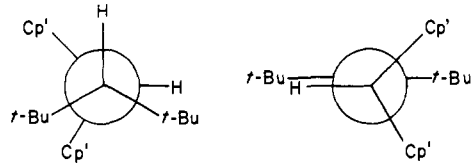

1e **1f**

that the lowest energy conformer is one in which the *t*-Bu groups lie near (**1e**) or in (**1f**) the "equatorial girdle" (the plane defined by Th, H, and O) in order to reduce unfavorable interactions with the Cp′ rings. Thus, the resulting lack of symmetry mirror planes requires magnetically nonequivalent *t*-Bu groups (**1e** and **1f**) and Cp′ rings (**1e**). Although the variable-temperature ^1H NMR spectra of the alkyl complexes $Cp'_2Th(R)(OCH\text{-}t\text{-}Bu_2)$ was not investigated, the observation of broadened *t*-Bu resonances at ambient temperature suggests that hindered rotation is occurring in these complexes as well and with similar energetic barriers.

Migratory Insertion of CO into Thorium–Carbon Bonds. Synthesis. Except for **1a**, the colorless alkyls synthesized above can be carbonylated smoothly and quantitatively at low temperatures and 1 atm of CO to produce the bright yellow acyls **5a–d** (eq 16). Upon prolonged exposure to CO or elevated temperatures

$$Cp'_2Th(R)(OR') + {}^*CO \rightarrow Cp'_2Th(\eta^2\text{-}{}^*COR)(OR') \quad (16)$$

5a, R = Me, R′ = CH-*t*-Bu$_2$; **5a***, *C= ^{13}C;

5b, R = *n*-Bu, R′ = CH-*t*-Bu$_2$; **5b***, *C = ^{13}C;

5c, R = CH_2-*t*-Bu, R′ = *t*-Bu; **5c***, *C = ^{13}C;

5d, R = CH_2-*t*-Bu, R′ = CH-*t*-Bu$_2$; **5d***, *C = ^{13}C

(≥25 °C), complex **1a** reacts further to form a host of products (as determined by NMR). The intense purple color of the resulting solution is reminiscent of that observed for the enedionediolate C formed via a η^2-acyl/CO coupling reaction,[26] suggesting

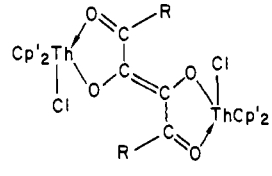

C

(25) Fagan, P. J. Ph.D. Thesis, Northwestern University, Evanston, IL, 1981.

(26) (a) Fagan, P. J.; Manriquez, J. M.; Marks, T. J.; Day, V. W.; Vollmer, S. H.; Day, C. S. *J. Am. Chem. Soc.* **1980**, *102*, 5393–5396. (b) Moloy, K. G.; Marks, T. J.; Day, V. W. *J. Am. Chem. Soc.* **1983**, *105*, 5696–5698. (c) Moloy, K. G.; Day, V. W.; Marks, T. J., submitted for publication.

Table I. $^{13}C\{^1H\}$ NMR and IR Data for Thorium η^2-Acyls and η^2-Formyls

complex	$^{13}C\{^1H\}$,[a] δ	ν_{CO} ($\nu_{^{13}CO}$),[b] cm^{-1}
5a	361.5	
5b	356.6	1479 (1447)
5c	361.9	1472 (~1443)[c]
5d	359.5	1452 (1434)
$Cp'_2Th(Cl)(\eta^2\text{-}COCH_2\text{-}t\text{-}Bu)$	360.2	1469 (1434)[d]
$Cp_3Th(\eta^2\text{-}COCH_2\text{-}t\text{-}Bu)$	356.7	1492[e]
8a	372	1477 (1443)[f]
8b	360	

[a] Measurements were made in C_6D_6 and referenced to internal Me_4Si. [b] Nujol or Fluorolube mulls. [c] The presence of several overlapping bands precludes a precise assignment. [d] Reference 26. [e] Reference 12b. [f] THF solution <−50 °C.

that such a species could account for at least one of the secondary pathways. Another candidate for a secondary product is the enediolate D. Species of this type have been shown to form from

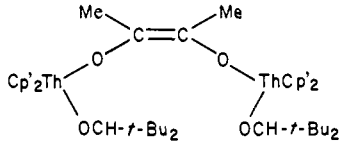

D

actinide alkyls and hydrides (vide infra) in the presence of carbon monoxide.[27] One possible product that may be ruled out, however, is the eneolate E, resulting from hydrogen atom migration in the

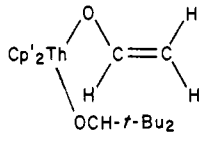

E

initially formed acyl. Chemistry of this type has been observed in our laboratories previously.[26] The apparent lack of resonances in the ^1H NMR spectrum assignable to such a species (an olefinic ABX pattern would be expected) seems to preclude such a possibility. After 24 h at 0 °C and 1 atm of CO, however, a ca. 40:60 mixture of **5a**/**1a** is obtained, thus allowing at least partial characterization of this complex.

Both infrared and ^{13}C NMR spectroscopies reveal parameters for **5a–d** characteristic of actinide η^2-acyls. The low-energy C–O stretching frequencies are typical of actinide η^2-acyls (see Table I).[28] Also, the $^{13}C\{^1H\}$ spectra of complexes **5a*–d*** reveal the characteristic low-field chemical shift for the acyl carbon atom (see Table I).[28] These data further complement the amply documented "oxycarbenoid" character (e.g., F ↔ G) of actinide[26a,28] and early transition-metal[29] η^2-acyls.

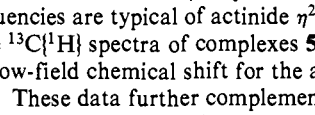

F G

Migratory Insertion of CO into Thorium–Hydrogen Bonds. Previous work in our laboratory and elsewhere has shown that actinide[4,27] and early transition-metal[29,30] hydrides may react with CO (or a metal carbonyl) to yield dimeric or trimeric products. A common mode of reactivity is depicted below (eq 17) wherein

$$2M\text{–}H + 2CO \rightarrow \textit{cis}\text{- or }\textit{trans}\text{-}MOCH{=}CHOM \quad (17)$$

CO is both reduced and coupled to form an enediolate ligand (vide supra). An obvious candidate as an intermediate in these processes would be a formyl complex, derived from a simple migratory insertion reaction. Thus, in order to hinder or nullify steps following the migratory insertion, which reasonably involve bimolecular reactions, we sought to synthesize very sterically hindered thorium hydrides such that the potential intermediate formyls could be observed or even isolated.

Indeed, the formation of cis-enediolates from thorium hydrides is impeded by the presence of bulky alkoxide groups. For instance, $Cp'_2Th(H)(O\text{-}t\text{-}Bu)$ (**6**) reacts with CO at 25 °C and 1 atm (as monitored by ^1H NMR) to produce the cis-enediolate **7a** in quantitative yield within a few minutes (eq 18). However, **1e**

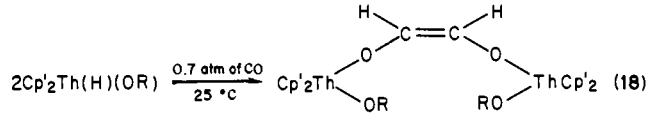

(18)

7a, R = *t*-Bu, $t_{1/2}$ ~ 3 min

b, R = CH-*t*-Bu$_2$, $t_{1/2}$ ~ 5 h

c, R = 2,6-*t*-Bu$_2$C$_6$H$_3$, no reaction

requires several hours for the reaction to reach completion and **1f** is unreactive under these conditions.[4] Even though this strategy did not result in the formation of an isolable formyl, the impeded rates of enediolate formation did allow the observation of such insertion products for hydrides **1e** and **1f**. Addition of CO (1 atm) to a colorless solution of either hydride in toluene-d_8 at −78 °C results in an immediate yellow coloration and CO uptake. Note that these color changes are very reminiscent of those observed in the carbonylation of the thorium alkyls discussed above, suggesting that formyls **8a,b** have indeed been generated (eq 19).

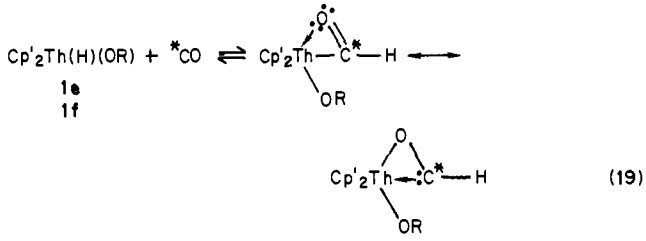

(19)

8a, R = CH-*t*-Bu$_2$, **8a***, C = ^{13}C

b, R = 2,6-*t*-Bu$_2$C$_6$H$_3$; **8b***, *C = ^{13}C

Supporting this hypothesis is the following spectroscopic evidence. First, low-temperature ^1H NMR spectra reveal resonances attributable to a new species with a very low field chemical shift (δ 15.2 for **8a**, δ 14.7 for **8b**), in addition to Cp′ and OR resonances in the proper intensity ratios (see Experimental Section for details). These low field shifts are common and characteristic of transition-metal formyls, generally spanning the region δ 17–12.[8] Furthermore, $^{13}C\{^1H\}$ NMR data obtained for **8a*** and **9b*** show singlets at δ 372 and 360, respectively. Note that these chemical shifts are characteristic of thorium η^2-acyls,[25,26] suggesting a similar structure (i.e., an "oxycarbene-like" η^2-formyl, cf. A ↔ B, above)

(27) Manriquez, J. M.; Fagan, P. J.; Marks, T. J.; Day, C. S.; Day, V. W. *J. Am. Chem. Soc.* **1978**, *101*, 7112–7114.

(28) (a) Marks, T. J.; Manriquez, J. M.; Fagan, P. J.; Day, V. W.; Day, C. S.; Vollmer, S. H. *ACS Symp. Ser.* **1980**, *No. 131*, 1–29. (b) Fagan, P. J.; Maatta, E. A.; Marks, T. J. *ACS Symp. Ser.* **1981**, *No. 152*, 53–78.

(29) Wolczanski, P. T.; Bercaw, J. E. *Acc. Chem. Res.* **1980**, *13*, 121–127 and references therein.

(30) (a) Manriquez, J. M.; McAlister, D. R.; Sanner, R. D.; Bercaw, J. E. *J. Am. Chem. Soc.* **1976**, *98*, 6733–6735. (b) Wolczanski, P. T.; Threlkel, R. S.; Bercaw, J. E. *J. Am. Chem. Soc.* **1979**, *101*, 218–220. (c) Manriquez, J. M.; McAlister, D. R.; Sanner, R. D.; Bercaw, J. E. *J. Am. Chem. Soc.* **1978**, *100*, 2715–2724. (d) Gell, K. I.; Schwartz, J. *J. Organomet. Chem.* **1978**, *162*, C11–C15. (e) Floriani, C.; Gambarotta, S.; Villa-Chiesi, A.; Guastini, C. *J. Am. Chem. Soc.* **1983**, *105*, 1690–1691. (f) Fachinetti, G.; Floriani, C.;f Roselli, A.; Pucci, S. *J. Chem. Soc., Chem. Commun.* **1978**, 269–270. (g) Kropp, K.; Skibbe, V.; Erker, G.; Krüger, C. *J. Am. Chem. Soc.* **1983**, *105*, 3353–3354. (h) Erker, G.; Kropp, K. *Chem. Ber.* **1982**, *115*, 2437–2446. (i) Erker, G.; Kropp, K.; Kruger, C.; Chiang, A.-P. *Chem. Ber.* **1982**, *115*, 2447–2460.

for the thorium formyls. In the ^{13}C NMR spectrum (proton coupled), each of these resonances appears as a doublet with $^1J_{C-H}$ = 114 (**8a***) and 117 Hz (**8b***). Also, the low field proton resonances are split into doublets with identical coupling constants. As a final test, selective heteronuclear decoupling experiments indicate that the respective low field ^1H and ^{13}C resonances constitute an AX spin system. The low values for $^1J_{C-H}$ appear to be typical of sp^2-hybridized carbons bonded to a transition metal.[8] Finally, low-temperature infrared spectra also support the structural assignment. In THF-d_8 solution (<−50 °C), a mixture of **1e** and CO exhibits, in addition to bands assignable to starting material, a shoulder at 1477 cm^{-1}. If the atmosphere is replaced with ^{13}CO and the system is allowed to equilibrate, the transition at 1477 cm^{-1} is observed to shift to 1443 cm^{-1}. These bands can be attributed to ν_{CO} (**8a**) and $\nu_{^{13}CO}$ (**8a***), respectively, and compare favorably with the parameters observed for actinide η^2-acyls.[25,26] The infrared isotopic shift is also in agreement with that predicted using Hooke's law. It should also be mentioned that no evidence for a metal carbonyl (ca. 2200–1800 cm^{-1}) was observed nor was a transition that could be unambiguously assigned to a formyl ν_{C-H}. The C–H stretch in aldehydes occurs at a characteristically low frequency (ca. 2750 cm^{-1}),[31] and absorptions at similar energies have been observed in d transition-metal formyls.[8] However, these bands are not necessarily diagnostic as they are often quite weak.[8] Also, it is not clear to what degree the thorium η^2-formyl is "aldehyde-like".

It was also discovered that the insertion reaction is rapid and reversible. As Figures 2 and 3 illustrate, varying the temperature causes substantial changes in the relative concentrations of hydride and formyl, with lower temperatures favoring the formyl. In addition, the bright yellow solutions (at −78 °C) became colorless upon warming to room temperature; these qualitative color changes are completely reversible. Moreover, addition of CO could be quantitatively reversed as determined by Toepler pump measurements, and the unreacted hydride recovered.

The remarkable rapidity of the carbonylation reaction is demonstrated in Figure 2. For CO insertion in complex **1e**, coalescence of hydride and formyl ^1H NMR resonances occurs at −45 °C. Analysis of these dynamic spectra by standard line shape equations[23,32] yields a rate constant at −45 °C for the forward reaction (k_f) of 8050 s^{-1} M^{-1} ($\Delta G_f^{\ddagger}$ = 9.2 ± 0.4 kcal/mol). Although Figure 3 shows that the rate of CO insertion into the Th–H bond of **1f** is not nearly as rapid as that found for **1e**, magnetization transfer studies indicate that formyl and hydride sites in **1f** and **8b** are indeed exchanging. Thus, irradiation of either ^1H resonance results in a partial collapse of the other. On the basis of these chemical and spectroscopic data, we therefore feel confident in ascribing these observations to reversible migratory CO insertion resulting in the formation of thorium η^2-formyls[33] (eq 19).

Thermodynamic Aspects of Thorium Hydride Carbonylation. From the temperature dependence of eq 19, it was possible to determine thermodynamic parameters for the migratory insertion process. The equilibrium constant was measured by NMR methods utilizing an NMR tube attached to a large gas reservoir, thus ensuring a constant, known CO pressure (Figure 1, see Experimental Section for details). Van't Hoff plots are shown in Figure 4, and the derived thermodynamic quantities for compound pairs **1e**,**8a** and **1f**,**8b** are compiled in Table II. These results show that the insertion process is in fact exothermic by approximately 5 kcal/mol. Although the data are not extensive, the apparent (albeit small) enthalpic differences between the two pairs could be attributed to the differing π-donating abilities of

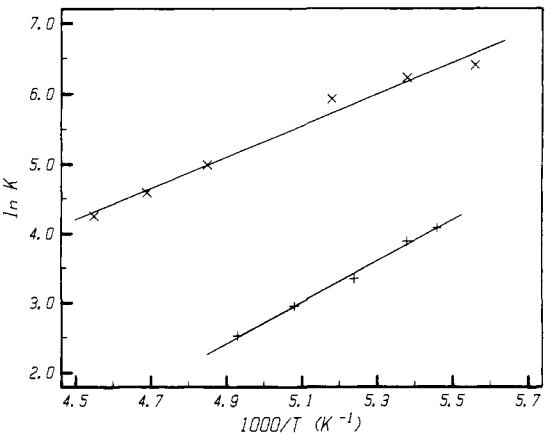

Figure 4. Van't Hoff plots for the hydride–formyl equilibrium as shown in eq 18 where x = **1e** and + = **1f**. The units of K are M^{-1}.

Table II. Thermodynamic Data for the Migratory Insertion of CO into Th–H Bonds To Yield η^2-Formyls

equilibrium	$\Delta H°$,[a] kcal/mol	ΔS,[a] eu
1e ⇌ **8a**	−4.5 ± 0.9	−11.7 ± 4.3
1f ⇌ **8b**	−5.9 ± 1.5	−23.9 ± 7.4

[a] Indicated errors represent 90% confidence limits.

alkoxide vs. aryl oxide. Since alkoxide is a superior π-donor, the Th(IV) center is rendered less oxophilic and hence the Th–(η^2-CHO) interaction is decreased relative to aryl oxide.[34] The greater steric bulk of the aryl oxide may account for the increased magnitude of the entropy term.

Also of interest is the value for K_H/K_D obtained via the double labeling experiment depicted in eq 20. K_H could be determined

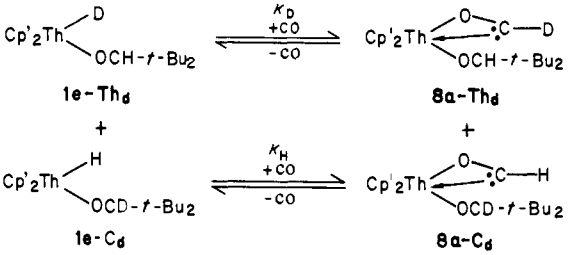

(20)

$$\frac{K_H}{K_D} = \frac{[\mathbf{8a}\text{-}C_d]/[\mathbf{1e}\text{-}C_d]}{[\mathbf{8a}\text{-}Th_d]/[\mathbf{1e}\text{-}Th_d]} = 0.31\ (5)\ \text{at}\ -78\ °C$$

by measuring the intensity of the formyl proton resonance (**8a**-C_d) relative to thorium hydride (**1e**-C_d). Likewise, the relative intensities of the alkoxide methine protons (**8a**-Th_d vs. **1e**-Th_d) yield a direct measure of K_D. This method allowed the simultaneous determination of both equilibrium constants under exactly the same conditions of CO pressure and temperature. At −78.5 ± 0.5 °C the value of K_H/K_D was found to be 0.31 (3). Because the thorium–hydrogen stretching vibration (1355 cm^{-1}) occurs at a much lower frequency than the formyl C–H vibration (presumably ~2800 cm^{-1}),[35d] a significant equilibrium isotope effect of less than unity is expected for the equilibrium as written.[35]

Mechanism of CO Insertion into Thorium–Ligand Bonds. For the present systems, either the stepwise (a) or concerted (b) pathways depicted in eq 21 seem the most plausible scenarios for migratory insertion.[1] In the first sequence, CO is proposed to first coordinate to the unsaturated metal center followed by migration of R to the resulting carbonyl (nucleophilic attack). It is known that for R = H, both steps are reversible whereas for R = alkyl, step 2 is irreversible. The major difference between this sequence and that typically observed for the carbonylation of transition-metal alkyls[1] (which usually bear ancillary carbonyl ligands) is

(31) Silverstein, R. M.; Bassler, G. C.; Morrill, T. C. "Spectrometric Identification of Organic Compounds", 4th ed.; Wiley: New York, 1981; p 120.

(32) (a) Anst, F. A. L.; Basus, V. J. *J. Magn. Reson.* **1978**, *32*, 339–343. (b) Shanan-Atidi, H.; Bar-Eli, K. H. *J. Phys. Chem.* **1970**, *74*, 961–963 and references therein.

(33) Note that there exist several examples of the insertion of isocyanides into metal–hydrogen bonds to yield iminoformyls: (a) Wolczanski, P. T.; Bercaw, J. E. *J. Am. Chem. Soc.* **1979**, *101*, 6450–6452. (b) Evans, W. J.; Meadows, J. H.; Hunter, W. E.; Atwood, J. L. *Organometallics* **1983**, *2*, 1252–1254.

(34) For similar effects in group 4B chemistry, see: Huffman, J. C.; Moloy, K. G.; Marsella, J. A.; Caulton, K. G. *J. Am. Chem. Soc.* **1980**, *102*, 3009–3014.

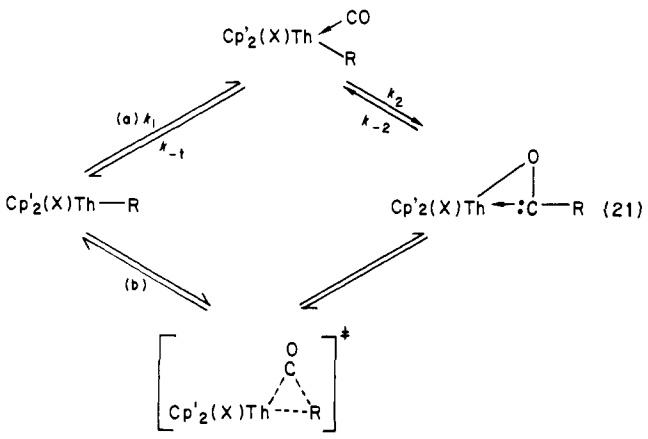

that in this case added CO ends up in the newly formed acyl ligand and not bound as a carbonyl. Although the concerted pathway (reversible for R = H; irreversible for R = alkyl) finds little precedent, the fact that Th(IV) carbonyls are as yet unknown[5,36] suggests that such an alternative should not be immediately dismissed.[37] Evidence for the various possibilities follows.

The rates and rate law for the carbonylation of alkyl **1b** were determined by gas-uptake measurements (see Experimental Section for details). Over a CO pressure range of 150–850 torr, the rate law was found to obey eq 22 (see Figure 5) where k'[CO]

$$\text{rate} = k'[\mathbf{1b}][\text{CO}] = kP_{\text{CO}}[\mathbf{1b}] \qquad (22)$$

$= kP_{\text{CO}}$, assuming Henry's law is obeyed. Thus, the kinetics for the insertion under the present conditions are consistent with either pathway a or b, and for path a, either k_1 or k_2 can be rate determining.

In order to elucidate the kinetics of thorium hydride carbonylation to yield the corresponding formyl, the following experiments were conducted. First, it was noted earlier that for eq 19 where R = CH-*t*-Bu_2, the CO insertion/extrusion was sufficiently rapid at low temperatures that the hydride and formyl proton resonances exhibit line broadening and eventually coalescence (Figure 2). By varying the initial concentration of **1e** while constant CO pressure/temperature are maintained and observing the spectral line widths near coalescence, it should be possible to deduce the reaction order in **1e**.[38] As Figure 6 shows, varying the concentration of **1e** by a factor of 5 causes a negligible change in the observed NMR line widths at half-height, consistent with a first-order dependence on metal hydride concentration and inconsistent with a rate-limiting intermolecular hydrogen transfer.[9] For the sample shown at −54 °C, the line broadening due to exchange for the formyl resonance (15.2 ppm) of **8a** (6.5×10^{-2} M) was found to be 19 ± 3 Hz (spectrum B). Upon a fivefold dilution the line width was found to be 16 ± 3 Hz (spectrum C). Had a bimolecular mechanism been operative, a fivefold dilution would have resulted in a line broadening of only 3–4 Hz.

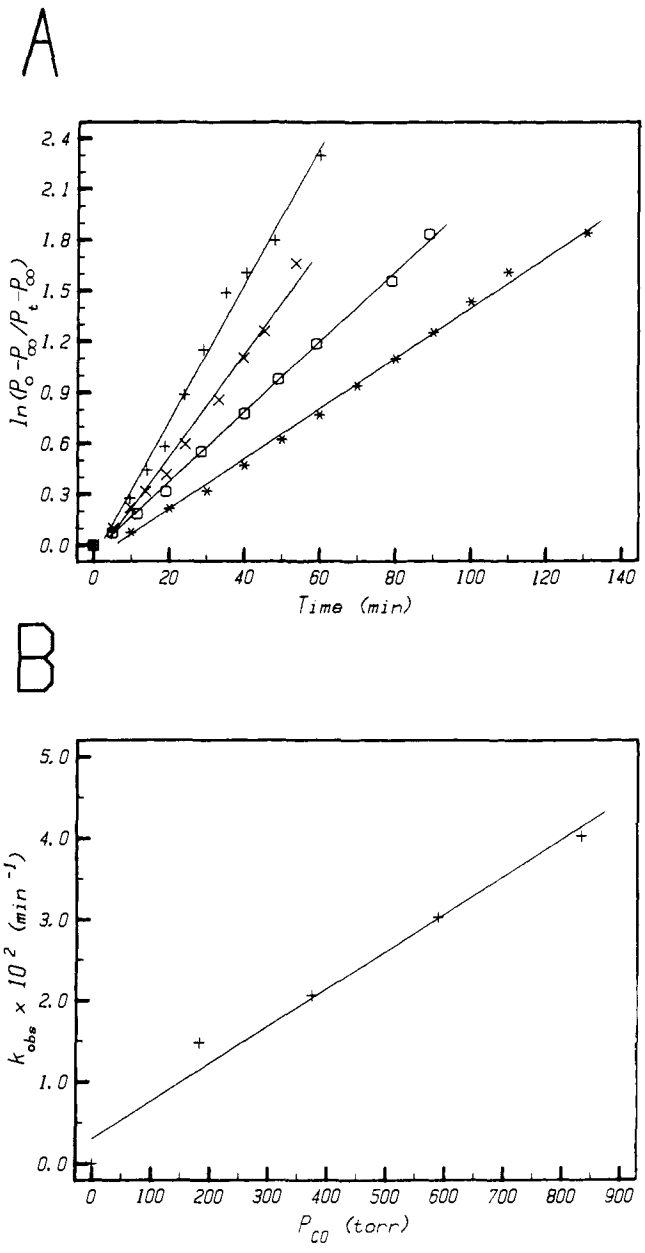

Figure 5. (A) Kinetic plots for the carbonylation of **1b** at various CO pressures: +, 833 torr; ×, 589 torr; O, 375 torr; *, 182 torr. (B) Dependence of the observed rate constants on CO pressure. From these data, $k = 4.6 \times 10^{-5}$ min^{-1} torr^{-1} at −54 ± 0.5 °C.

Labeling and crossover experiments lend further credence to the above results and to the formulation of the formyls as monomeric. Addition of CO to a mixture of **1e** and **1f** in toluene-d_8 at low temperature shows that only **8a** and **8b** are formed. If the formyls were in fact dimeric, it would reasonably be expected that mixed species such as **9c** would be detected (eq 23), along with

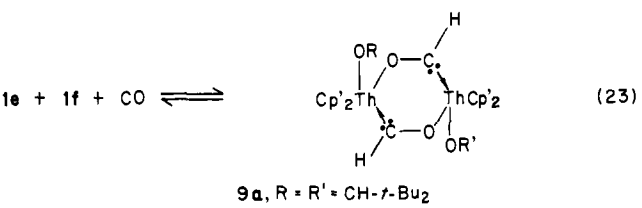

(23)

9a, R = R' = CH-*t*-Bu_2
b, R = R' = 2,6-*t*-Bu C_6H_3
c, R = CH-*t*-Bu_2, R' = 2,6-*t*-$Bu_2C_6H_3$

9a and **9b**; thus, three formyls would be observed (note that **9c**

(35) (a) More O'Ferrall, R. A. In "Proton-Transfer Reactions"; Caldin, E., Gold, V., Eds.; Chapman and Hall: London, 1975; Chapter 8. (b) Buddenbaum, W. E.; Shiner, V. J., Jr. In "Isotope Effects on Enzyme-Catalyzed Reactions"; Cleland, W. W., O'Leary, M. H., Northrop, D. B. Eds.; University Park Press: Baltimore, 1977; pp 1–36. (c) Wolfsberg, M. *Acc. Chem. Res.* **1972**, *5*, 225–233. (d) An admittedly simplistic calculation of the thorium formyl C–H stretching frequency based upon the equilibrium isotope effect and the differences in zero-point energies of the ThH/ThD-ThCHO/ThCDO stretching oscillators, $K_H/K_D = e^{-1[(\Delta_{\text{products}}-\Delta_{\text{reactants}})/kT]}$, yields a value of ca. 2500 cm^{-1}.

(36) Trivalent actinide carbonyls have been identified in cryogenic matrices and a d^0 Zr(IV) carbonyl has been observed in a low-temperature solution infrared study.[36a,b] Also, a recent theoretical investigation suggests that actinide carbonyls should be stable.[36c] (a) Hauge, R. H.; Grandsde, S. E.; Margrave, J. L. *J. Chem. Soc., Dalton Trans.* **1979**, 745–748. (b) Marsella, J. A.; Curtis, C. J.; Bercaw, J. E.; Caulton, K. G. *J. Am. Chem. Soc.* **1980**, *102*, 7244–7246. (c) Tatsumi, K.; Hoffmann, R. *Inorg. Chem.* **1984**, *23*, 1633–1634. We thank these authors for a preprint of their work prior to publication.

(37) Although the carbonylation of noncarbonyl-bearing alkyl complexes is assumed[1] to proceed via a mechanism involving CO precoordination (path a of eq 7), as yet there is no concrete evidence that this is, in fact, the case: Lauher, J. W.; Hoffmann, R. *J. Am. Chem. Soc.* **1976**, *98*, 1729–1742.

(38) (a) Ham, N. S.; Mole, T. In *NMR Spectrosc.* **1969**, *4*, 112. (b) Drago, R. S. "Physical Methods in Chemistry"; W. B. Saunders: Philadelphia, 1977; pp 257–259.

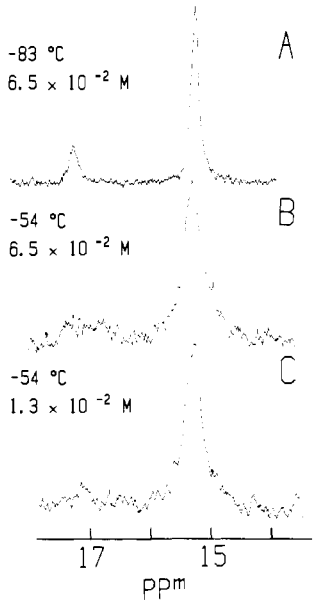

Figure 6. Dependence of the NMR line shapes for the equilibrium **1e** + CO ⇌ **8a** on hydride concentration. (A) NMR spectrum of a 6.5 × 10^{-1} M solution of **1e** in the presence of 1.16 atm of CO in the stopped-exchange region. The resonance at 15.2 ppm corresponds to **8a** and that at 17.2 ppm to **1e**. (B) The same sample after warming the probe to −54 °C to allow line broadening to occur. (C) The effect of a fivefold dilution on the NMR line widths.

would exhibit two formyl resonances). Furthermore, molecular models and the fact that the hydrides exhibit hindered rotation of the alkoxide groups (vide supra) argue that severe steric repulsions would render such a structure prohibitively high in energy. Furthermore, experiments involving the addition of CO to 1:1 solutions of **1e-Th$_d$** and **1f** (eq 24) reveal that *only* (≥97%) **8a-Th$_d$**

$$\textbf{1e-Th}_d + \textbf{1f} \overset{CO}{\rightleftharpoons} \textbf{8a-Th}_d + \textbf{8b} \qquad (24)$$

and **9b** are formed and no cross labeling is observed over the course of several hours at −58 °C. On a shorter timescale, magnetization transfer labeling experiments on a mixture of **1e**/**8a** and **1f**/**8b** also reveal that detectable hydrogen atom permutation only occurs between metal hydride and metal formyl containing the same alkoxide ligand. These results reasonably rule out intermolecular

Table III. Kinetic Data for $Cp'_2Th(R)(X)$ Migratory CO Insertion

compd			
R	X	temp, °C	k, min^{-1} $torr^{-1}$
H	OCH-*t*-Bu_2	−45	3.0 (3)
CH_2-*t*-Bu	Cl	−54	4×10^{-2}
CH_2-*t*-Bu	O-*t*-Bu	−54	4×10^{-3}
CH_2-*t*-Bu	OCH-*t*-Bu_2	−54	6×10^{-4}
n-Bu	OCH-*t*-Bu_2	−54	$4.6\ (7) \times 10^{-5}$
Me	OCH-*t*-Bu_2	0	5×10^{-7}

hydride transfer (even if the bimolecular component is not rate-limiting) as in eq 25, since it seems highly unlikely that such

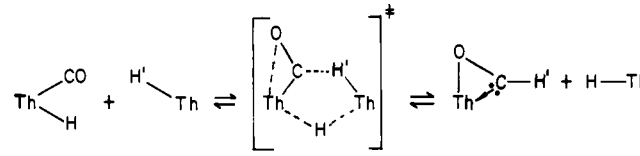

(25)

processes would occur exclusively for reactant pairs with the same alkoxide functionality. Note that both of the reactions depicted in eq 23 and 25 are inconsistent with the variable concentration line-broadening experiments discussed above as well. Therefore, it appears that both alkyl and hydride CO insertions follow one of the pathways in eq 21.

The kinetic data cannot distinguish between paths a and b in eq 21 nor is it possible to determine, with the data presented thus far, whether k_1 or k_2 in path a is rate limiting. It was, however, possible to design an experiment to show that if path a is operative, k_2 is indeed rate limiting by the demonstration that the insertion process for thorium hydrides exhibits a substantial primary kinetic isotope effect. This effect was measured via the double-labeling experiment depicted in eq 20. Recall that for the equilibrium depicted, the insertion is rapid enough at low temperature to cause significant NMR line broadening and eventual coalescence (at ca. −45 °C) of hydride and formyl resonances. Thus, analysis in the slow to intermediate exchange regions of the alkoxide methine proton line shapes[23] in complexes **1e-Th$_d$** and **8a-Th$_d$** yields values for $(k_D)_{forward}$ and $(k_D)_{reverse}$. Likewise, the broadened hydride (**1e-C$_d$**) and formyl (**8a-C$_d$**) resonances yield values for $(k_H)_{forward}$ and $(k_H)_{reverse}$, respectively. Again, this double-labeling experiment allowed the simultaneous determination of all rate data under exactly the same conditions of CO pressure and temperature.

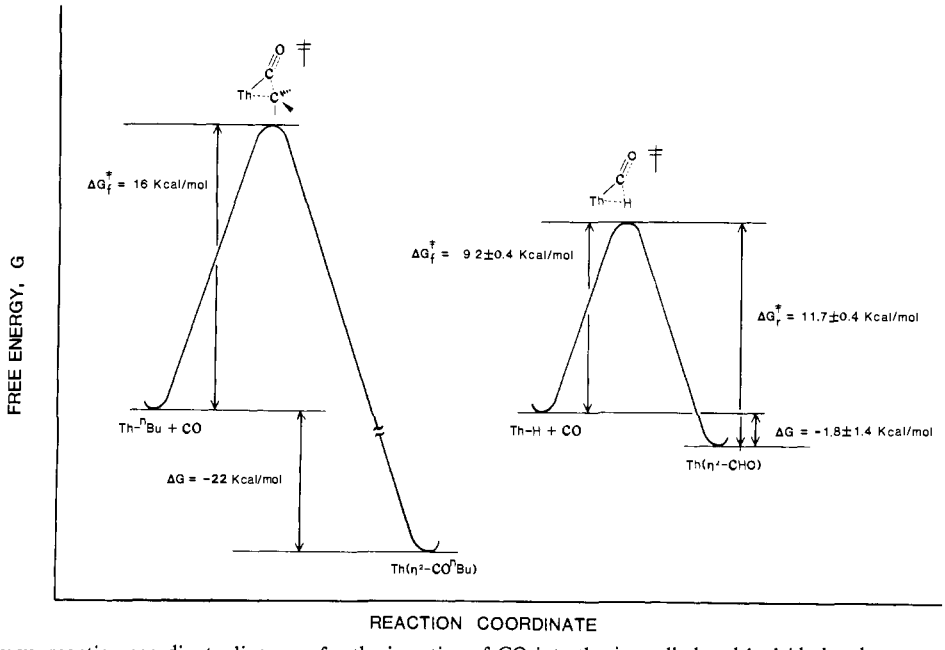

Figure 7. Free energy vs. reaction coordinate diagrams for the insertion of CO into thorium alkyl and hydride bonds at ca. −50 °C. The positions of the reactants have been arbitrarily placed at the same energy level. Also, because it was not possible to determine the energetic positions of the presumed alkyl and hydride carbonyl intermediates (Th(CO)(R)), these preequilibria have been omitted.

Thus, at −58 °C $(k_H/k_D)_{forward} = 2.8$ (4) and $(k_H/k_D)_{reverse} = 4.1$ (5).[39] As a check on the above result, it should be noted that the ratios of the forward to reverse kinetic isotope effects is simply K_H/K_D, the equilibrium isotope effect. For the above results, this yields $K_H/K_D = 0.68$ (20). At −78 °C, K_H/K_D was found to be 0.31 (5) by direct integration methods (vide supra). Thus, given the error limits in the derived values ($\Delta/\sigma = 1.9$) and the fact that the measurements were carried out at slightly different temperatures,[40] these results appear to be internally consistent. Since the transition state in step 2 of path a may be indistinguishable from that postulated for bath b, neither mechanism can be ruled out. Importantly, however, these results demonstrate that for any mechanism invoked, the rate-determining step must involve hydride migration. The magnitude of $(k_H/k_D)_{forward}$ is consistent with a highly unsymmetrical and/or nonlinear transition state,[35] as might be expected for such a migratory insertion.

Finally, the present data give no indication as to the precise disposition of the ligands about thorium during the carbonylation reaction (e.g., H vs. I in eq 26). The molecular structure of

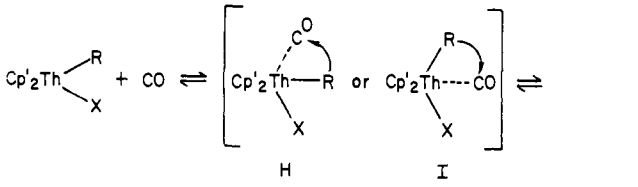

H I

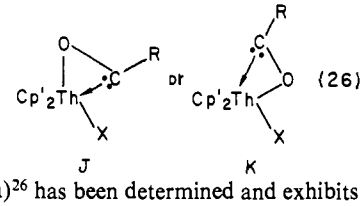

J K (26)

$Cp'_2Th(Cl)(\eta^2\text{-}COCH_2\text{-}t\text{-}Bu)$[26] has been determined and exhibits configuration J. Similar d element complexes (e.g., $Cp'_2Zr(R)(\eta^2\text{-}COR)$) have been shown to adopt the opposite configuration (K) although J may be the kinetic product in this transformation.[37a,41] Recent work[6] with actinide η^2-carbamoyls suggests that the energy barrier between either configuration may be quite small ($\Delta G^{\ddagger} \approx 10$ kcal/mol at −80 °C). In the present work, only one isomer for each acyl or formyl was detected by NMR.

Migratory Aptitudes of Alkyl and Hydride Ligands. Before the relative migratory aptitudes of the alkyls and hydrides investigated herein can be discussed, it is necessary to first examine what has been learned concerning the mechanism of the reaction. If pathway b in eq 21 is operative, then the measured rate constants provide a direct measure of the ligand migratory aptitudes. However, if path a is operative, the situation becomes more complex. For R = alkyl, it is known that k_{-2} is negligible and, after a steady-state approximation is applied to the intermediate carbonyl, the rate law is given by eq 27. Thus, the measured

$$\text{velocity} = k_2(k_1/k_{-1})[\text{ThR}][\text{CO}] = kP_{CO}[\text{ThR}] \quad (27)$$

rate constant is a composite of the migratory insertion (k_2) and a preequilibrium (k_1/k_{-1}). Only k_2 yields information concerning migratory aptitudes. Since no carbonyls were observed by infrared spectroscopy for the carbonylation of **1e**, it can be estimated that $k_1/k_{-1} < 10\ M^{-1}$ at −65 °C with use of published CO infrared extinction coefficients.[42] Although this calculation yields an upper limit for k_1/k_{-1}, it in no way determines or predicts how the preequilibrium will change with the steric and electronic properties of the R and X substituents on thorium. Nevertheless, in order to obtain at least a rough ranking of migratory aptitudes, a series of complexes of the type $Cp'_2Th(R)(OCH\text{-}t\text{-}Bu_2)$ (R = H, CH_2-*t*-Bu, *n*-Bu, Me) was synthesized in an effort to maintain a constant steric and electronic influence about the metal as a result of the ancillary ligands (Cp′, $OCH\text{-}t\text{-}Bu_2$) present.

For the series of complexes examined, it was found that hydride insertion is always much more rapid than alkyl insertion (see Table III). For instance, hydride insertion was found to be ca. 10^8 times faster than methyl insertion and even the most reactive alkyl, neopentyl, underwent migratory insertion 5×10^3 times more slowly than the corresponding hydride. On the basis of the discussion above, the greater rapidity of hydride vs. alkyl insertion cannot be interpreted in terms of the relative thermodynamics of the insertion process. Had the energy of the transition state been governed by ground-state parameters, the observed kinetic ordering hydride > alkyl would be reversed since thorium–hydrogen bond disruption enthalpies exceed those of thorium–carbon bonds by approximately 15 kcal/mol.[15,43] Furthermore, thorium alkyl carbonylation is significantly more exothermic than thorium hydride carbonylation.[15] Thus, it is concluded that the reduced barrier for hydride migratory insertion is a kinetic property of the migrating group. A similar trend has been observed in the relative rates of carbene insertion depicted in eq 28.[9] Here hydride

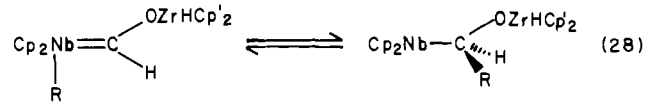

(28)

migration was observed to be ca. 5×10^4 times faster than methyl migration. The same argument used to explain this result may be applied to the formyl/acyl case. Basically, hydride forms more stable three-center, two-electron bonds than sp^3 carbon as a result of the highly symmetrical s valence orbital. Thus, a transition state such as L is predicted to lie at lower energy relative to the

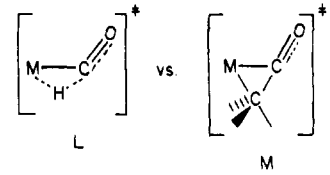

L vs. M

ground state than M (note that this argument applies whether path a or path b of eq 21 is operative). This trend (hydride migrates faster than alkyl) also parallels that observed in carbonium ion rearrangements (e.g., pinacol and Wagner–Merwein rearrangements). Very roughly, the similarity here can be viewed in terms of the migration of an alkyl or hydride ligand to the empty π^* orbital on the carbonyl carbon atom in N relative to the

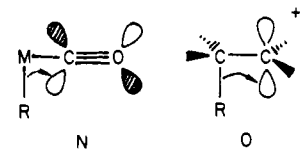

N O

analogous migration to the empty sp^2 orbital on the adjacent carbenium ion in O.[44] Finally, it should be pointed out that one

(39) Indicated errors correspond to 1 esd.

(40) Due to the inherent error in integrating exchange-broadened resonances, the value for K_H/K_D at −78 °C, rather than −58 °C, is quoted. At −58 °C, however, the value for K_H/K_D is estimated to be 0.36 (14) and thus remains consistent with our argument. Also, the temperature dependence of the isotope effects was not measured for two reasons. First, such changes with temperature are typically rather small and the measured esd's for the effects measured in this paper are unavoidably large. Second, at higher temperatures (>−40 °C) the ^1H NMR spectrum in the alkoxide methine region (δ 4.0–3.5) becomes complicated with as yet unidentified resonances and consequently limits the temperature range of such a measurement to ca. 30 °C.

(41) (a) Fachinetti, G.; Floriani, C.; Stoeckli-Evans, H. *J. Chem. Soc., Dalton Trans.* **1977**, 1946–1950. (b) Fachinetti, G.; Floriani, C. *J. Organomet. Chem.* **1974**, *71*, C5–C7. (c) Erker, G.; Rosenfeldt, F. *Angew. Chem., Int. Ed. Engl.* **1978**, *17*, 605–606. (d) Erker, G.; Rosenfeldt, F. *J. Organomet. Chem.* **1980**, *188*, C1–C4. (e) **Note Added in Proof**: Diffraction studies show that $Cp'_2Th(Cl)(\eta^2\text{-}COC_6H_5)$ adopts structure K in the solid state (Liang, W.-B.; Marks, T. J., unpublished results).

(42) Kettle, S. F. A.; Paul, I. *Adv. Organomet. Chem.* **1972**, *10*, 199–236.

(43) Gas-phase bond disruption enthalpies (*D*) in kcal/mol, for the series of complexes $Cp'_2Th(R)(O\text{-}t\text{-}Bu)$ follows: R = Me, *D* = 79.3 (1.2); R = CH_2-*t*-Bu, *D* = 77.9 (3.4); R = *n*-Bu, *D* = 73.9 (3.7). For **1e** and **1f** *D*(Th–H) = 86.8 (1.5) and 84.9 (1.3) kcal/mol, respectively.[15]

(44) (a) Saunders, M.; Chandrasekhar, J.; Schleyer, P. von R. In "Rearrangements in Ground and Excited States", de Mayo, P., Ed.; Academic Press: New York, 1980; Essay 1. (b) Pocker, Y. In "Molecular Rearrangements"; de Mayo, P., Ed.; Interscience: New York, 1963; Chapter 1. (c) Carey, F. A.; Sandberg, R. J. "Advanced Organic Chemistry"; Plenum Press: New York, 1978, p 236. (d) March, J. "Advanced Organic Chemistry"; McGraw-Hill: New York, 1968; p 787.

theoretical study[45] has predicted that hydride migration to a bound carbonyl ligand should be more facile than methyl migration. Here the computed difference in activation energy was found to be 0.15 eV, corresponding to a difference in the rate of migratory insertion of ca. 3.5×10^2. This stabilization of the formyl transition state was attributed to a lowering of the orbital that evolves into the new C–H bond.

Within the group (albeit small) of alkyl complexes examined in the present study it is noted that in general the rate of acyl formation is increased by bulky alkyls (i.e., CH_2-*t*-Bu > *n*-Bu > Me; see Table III). On the basis of published thermodynamic data,[15] this kinetic ordering only partially reflects the relative bond strengths of the alkyls employed in this study. If the alkyl migration rates were strongly correlated with the strength of the metal–carbon bond being broken, the ordering *n*-Bu $\gtrsim$ CH_2-*t*-Bu > Me would have been expected.[43] The same bulky alkoxide functionality (–OCH-*t*-Bu_2) was employed in order to ensure nearly equivalent comparisons. This phenomenon (bulky alkyls accelerate the rate of insertion) has been noted before in both d[1,46] and f element[12b] systems and will not be dealt with in detail here. It is interesting to note, however, that the reaction rate is apparently decreased by the presence of a bulky alkoxide group. Thus, complex **1c** undergoes carbonylation approximately 6 times more rapidly than **1d**. Also, comparison of Figures 2 and 3 shows that complex **1f** inserts CO less rapidly than does **1e**, presumably a result of the increased steric bulk of the 2,6-disubstituted phenoxide ligand, even though formation of **8b** is slightly more exothermic than that of **8a** (vide supra). Although this result is difficult to interpret on the basis of the argument just presented (bulky alkyls accelerate the carbonylation), we suspect that the possibility the measured rate constants are actually a composite of a kinetic preequilibrium followed by a rate-determining migratory insertion (vide supra) may account for this small but noticeable discrepancy.

Finally, it is noted that the presence of a halide ligand (Cl) in place of alkoxide results in a further increase of the reaction rate. For the present case, $Cp'_2Th(CH_2$-*t*-Bu)(Cl) undergoes carbonylation 12 times faster than complex **1c**. This observation may be explained in terms of either steric or electronic effects. First, chloride is smaller than *tert*-butoxide (which in turn is smaller than –OCH-*t*-Bu_2), and evidence has already been presented that suggests that a small X group in $Cp'_2Th(R)(X)$ may enhance carbonylation. Second, since chloride is a poorer electron donor than alkoxide, the thorium (IV) center is formally more unsaturated in the halide complex.[34] Thus, addition/insertion of a nucleophile, in this case CO, is expected to be more rapid. Alternatively, the Th–C bond is weakened by chloride,[15] relative to alkoxide, thus facilitating the migration. This result is substantiated by the observation that $Cp_2Zr(Me)(Cl)$ is smoothly carbonylated under 1 atm of CO whereas $Cp_2Zr(Me)(OEt)$ is inert under these conditions.[47]

Discussion

This study offers support for the postulate that the stoichiometric migratory insertion of CO into a metal–hydrogen bond is, in general, limited by thermodynamic rather than kinetic constraints. Although the predicted results may vary about the periodic table, it is now generally believed that for middle and late metals of the first transition series, CO migration into a metal–hydrogen bond is endothermic.[8,48] Estimates of the endothermicity vary from 5 to 20 kcal/mol and may be compared with the exothermic (–8 to –14 insertion of CO into a metal–alkyl bond. As several workers have pointed out,[48] the major contributing factor to this difference lies in the fact that metal–hydrogen bonds are "stronger" (i.e., have greater bond disruption enthalpies) than metal–carbon bonds by up to 30 kcal/mol. Thus, to a first approximation, the formation of the formyl metal–carbon bond is thermodynamically insufficient to compensate for the disruption of the metal–hydrogen bond.

Recent results in this laboratory[15] suggest that the difference between thorium hydride and thorium alkyl bond disruption enthalpies is only on the order of ca. 15 kcal/mol. One attractive explanation[15c] for this rather small difference derives from the high polarity of actinide-ligand bonds.[5,6] The more polarizable alkyl ligand can stabilize negative charge more effectively than the hydride ligand.

$$M^{\delta+}—CH_3^{\delta-} \qquad M^{\delta+}—H^{\delta-}$$

If this D(Th–CH_3) vs. D(Th–H) relationship is factored into the hydride/formyl equilibrium of eq 19, it can be estimated that this equilibrium is approximately thermoneutral, before the thorium–oxygen interaction is taken into account. Of course, this argument leads to the conclusion that the thorium–formyl oxygen bond strength only amounts to 5 kcal/mol or so, clearly an underestimate. For example, the thorium–oxygen bond length in $Cp'_2Th(Cl)(\eta^2$-$COCH_2$-*t*-Bu) is 2.37 (2) Å.[26a] This value is only slightly longer than the Th–O single bond distance in $\{Cp'_2Th[\mu$-$OC(CH_3)C(CH_3)O]\}_2$, 2.150 (4) Å.[28] Also, it can be estimated that thorium, being a very oxophilic metal, will form bonds with oxygen that are ca. 50 kcal/mol stronger than those with carbon.[15,28] Thus, a substantial Th–O interaction is indicated. Although it is difficult to partition the Th–C and Th–O bond energy contributions in the η^2-formyl, the exothermicity of the insertion is clearly accounted for.

On a more general level, assessing how the thermodynamics of eq 1 for R = H are influenced by D(M–C) vs. D(M–H) relationships as well as by coordinative unsaturation and/or oxophilicity (which may promote η^2-CHO ligation) is hampered by a paucity of thermochemical and structural data. In the case of the aforementioned, formally 16-electron rhodium porphyrinato systems[7] (eq 3), $\Delta H = -13$ kcal/mol,[51] and the formyl bonding has been shown unambiguously to be of the η^1 type.[7] Thus, it is apparent that D(Rh–H) – D(Rh–C) has decreased by perhaps 20 kcal/mol from that which might be expected for a more conventional group 8 complex. An example that bears a closer resemblance to thorium hydride carbonylation chemistry is shown in eq 29.[30f] Here, addition of CO to $Cp_2Zr(H)(Cl)$ (formally

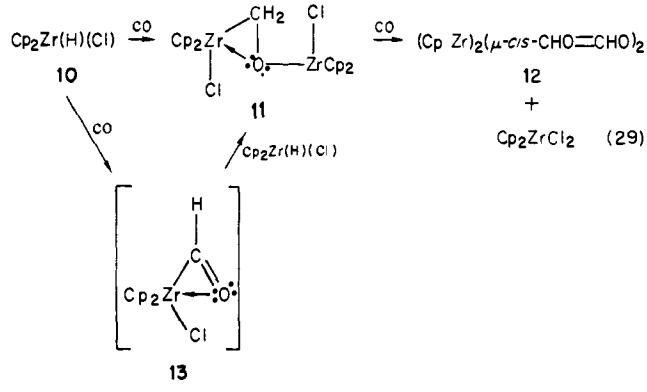

a 16-electron system) results in the formation of an isolable oxymethylene intermediate, **11**, which undergoes further carbonylation to yield a dimeric, cis-enediolate complex (**12**). The intermediacy of a formyl (**13**) in this reaction seems reasonable in

(45) Berke, H.; Hoffmann, R. *J. Am. Chem. Soc.* **1978**, *100*, 7224–7236.
(46) Cotton, J. D.; Crisp, G. T.; Latif, L. *Inorg. Chim. Acta* **1981**, *47*, 171–176 and references therein.
(47) Marsella, J. A.; Moloy, K. G.; Caulton, K. J. *J. Organomet. Chem.* **1980**, *201*, 389–398.
(48) (a) Halpern, J. *Acc. Chem. Res.* **1982**, *15*, 238–244 and references therein. (b) Halpern, J. *Pure Appl. Chem.* **1979**, *51*, 2171–2182. (c) Connor, J. A.; Zafarani-Moattar, M. T.; Bickerton, J.; Saied, N. I.; Suradi, S.; Carson, R.; Takhin, G. A.; Skinner, H. A. *Organometallics* **1982**, *1*, 1166–1174 and references therein. (d) Connor, J. A. *Top. Curr. Chem.* **1977**, *71*, 71–110.
(49) (a) Bruno, J. W.; Fendrick, C. M.; Smith, G. M.; Marks, T. J., manuscript in preparation. (b) Fendrick, C. M.; Marks, T. J.; Day, V. W. *Organometallics* **1984**, *3*, 819–821.
(50) Pauling, L. "The Nature of the Chemical Bond", 2nd ed.; Cornell University Press: Ithaca, NY, 1960; p 224.
(51) Woods, B. A.; Wayland, B. B.; Minda, V. M.; Duttahmed, A. Abstracts, 185th National Meeting of the American Chemical Society, Seattle, WA, Mar 1983; American Chemical Society: Washington, DC, 1983; INOR 144.

view of the present results and earlier work in our laboratory which demonstrated that an analogous pathway is likely traversed by actinide hydrides to yield enediolates (cf. eq 18).[27a] A few other zirconium complexes display similar reactivity.[30]

A second important fact derived from the present study is that hydride is a far superior migrating group to alkyl. Thus, even if the insertion is slightly endothermic (and, therefore, the formyl intermediate is not isolable or observable), the rapidity of the migration suggests that formyls may play a role as pivotal and, therefore, kinetically important, intermediates in various transformations involving bound carbon monoxide. This possibility has been discussed by other workers to account for substitution and isomerization processes of certain metal carbonyl hydrides.[52] In an equal vein, the results presented herein are of paramount mechanistic importance to several technologically important syngas conversions (both homo- and heterogeneous). Of particular relevance are those in which the carbon–oxygen bond of the CO molecule is at least partially retained in the product (i.e., methanol, ethylene glycol, aldehydes, formates, etc.).[2,3] Of these, the heterogeneous ZnO-catalyzed synthesis of methanol from CO and hydrogen provides some of the best evidence for the intermediacy of formyls during the reduction process.[2b] Surface spectroscopic studies (infrared and photoemission) have yielded substantial evidence for hydride,[53] hydroxide,[53] carbonyl,[53b] methoxide,[54] and, more recently, formyl[55] species on ZnO after exposure to CO/H_2 mixtures. Recently we presented kinetic evidence that suggested that the conversion of hydride **1e** to the corresponding methoxide (eq 30) in the presence of CO and hydrogen proceeded through the formyl **8a**.[27a] Clearly, this result coupled with the evidence above suggests that formyls are plausible intermediates in heterogeneous methanol synthesis.

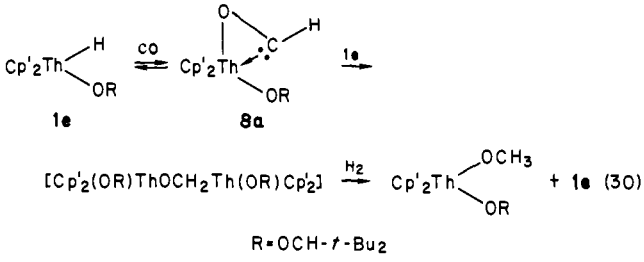

The present results are also of relevance to the homogeneous cobalt-catalyzed reduction of syngas to oxygenates. The observed zero-order dependence on CO pressure and an apparent inverse kinetic isotope effect ($k_H/k_D = 0.73$) with the use of deuterium gas has led workers in this field to suggest a formyl as an intermediate.[3a,b,g,h] The experimental observations were deemed to be consistent with a rapid, reversible preequilibrium in which hydrogen migration occurs to yield a formyl followed by a rate-determining addition of dihydrogen (eq 31). Herein we provide

$$HCo(CO)_4 \overset{\text{fast}}{\rightleftharpoons} (CO)_3Co\text{–}CHO$$

$$(CO)_3Co\text{–}CHO + H_2 \xrightarrow{\text{rds}} (CO)_3H_2Co\text{–}CHO \rightarrow \text{products} \quad (31)$$

the only conclusive support for this postulate. Namely, the hydride insertion reaction can be, in fact, extremely rapid, and the formyl equilibrium does display a significant thermodynamic isotope effect. Thus, since deuterium substitution favors the right side of the formyl equilibrium, an apparent inverse kinetic isotope effect is observed for the reaction shown in eq 31.

Finally, it is possible to compare the energy profiles of hydride and alkyl (in this case *n*-Bu) migratory insertion. From the rate data obtained in this study, it is possible to calculate an approximate $\Delta G^{\ddagger}$ for each reaction. From the NMR data shown in Figure 2, $\Delta G_f^{\ddagger}$ at coalescence (−45 °C) was found to be 9.2 ± 0.4 kcal/mol and $\Delta G^{\ddagger}_r = 11.7 \pm 0.4$ kcal/mol for hydride migration.[32] From the rate of CO insertion in complex **1b**, $\Delta G_f^{\ddagger}$ is estimated to be ca. 16 kcal/mol at −54 °C. The enthalpy contribution to acyl formation (ΔH) has been determined to be −29.5 (2.3) kcal/mol for $Cp'_2Th(n\text{-Bu})(OCH\text{-}t\text{-}Bu_2)$.[56] If it is assumed that the entropy contribution (ΔS) to this process is similar to the value of 33 eu obtained for $Cp_2Hf(Me)_2$ carbonylation to yield $Cp_2Hf(\eta^2\text{-COMe})(Me)$,[1c] ΔG for thorium acyl formation is calculated to be ca. −8 kcal/mol at −54 °C. These data are depicted graphically in Figure 7 and show that the hydride/formyl potential energy surface is much flatter than the corresponding alkyl/acyl case. Although this picture may be altered somewhat in d metal systems, we believe that the overall result that the formyl formation is usually limited by thermodynamic effects and that the kinetic ordering H >> alkyl will still hold.

Acknowledgment. This research was supported by the National Science Foundation under Grants CHE8009060 and CHE8306255. K.G.M. thanks Dow Chemical Co. for a fellowship.

Registry No. **1a**, 91742-32-4; **1b**, 91742-33-5; **1c**, 91742-34-6; **1d**, 91742-35-7; **1e**, 79932-08-4; **1e-Th$_d$**, 91742-36-8; **1e-C$_d$**, 91742-37-9; **1f**, 79932-09-5; **2**, 79301-21-6; **4**, 67506-92-7; **5a**, 91742-38-0; **5a***, 91742-39-1; **5b**, 91759-09-0; **5b***, 91742-40-4; **5c**, 91742-41-5; **5c***, 91742-42-6; **5d**, 91742-43-7; **5d***, 91742-44-8; **8a**, 79932-04-0; **8a-C$_d$**, 91742-45-9; **8a-Th$_d$**, 91742-46-0; **8a***, 79932-05-1; **8b**, 79932-06-2; **8b***, 79932-07-3; $Cp'_2Th(Cl)(\eta^2\text{-}COCH_2\text{-}t\text{-Bu})$, 74587-36-3; $Cp'_2Th(Cl)(CH_2\text{-}t\text{-Bu})$, 74587-39-6; $Cp'_2Th(Cl)(O\text{-}t\text{-Bu})$, 79301-33-0; $Cp'_2Th[CH_2C(CH_3)_2CH_2]$, 83692-52-8; $[Cp'_2Th(\mu\text{-D})(D)]_2$, 79301-32-9; Cp'_2ThCl_2, 67506-88-1; Cp'_2ThMe_2, 67506-90-5; $Cp'_2Th(n\text{-Bu})_2$, 86727-40-4; $t\text{-Bu}_2CO$, 815-24-7; CO, 630-08-0.

(52) (a) Davies, S. G.; Simpson, S. J. *J. Organomet. Chem.* **1982**, *240*, C48–C50. (b) Davies, S. G.; Hibberd, J.; Simpson, S. J. *J. Chem. Soc., Chem. Commun.* **1982**, 1404–1405. (c) Pearson, R. G.; Walker, H. W.; Mauermann, H.; Ford, P. C. *Inorg. Chem.* **1981**, *20*, 2743–2745. (d) Richmond, T. G.; Basolo, F.; Shriver, D. F. *Organometallics* **1982**, *1*, 1624–1628.

(53) (a) Dent, A. L.; Kokes, R. J. *J. Phys. Chem.* **1969**, *73*, 3781–3790. (b) Boccuzzi, F.; Borello, E.; Zecchina, A.; Bossi, A.; Camia, B. *J. Catal.* **1978**, *51*, 150–159. (c) Mehta, S.; Simmons, G. W.; Klier, K.; Herman, R. G. *J. Catal.* **1979**, *57*, 339–346. (d) D'Amico, K. L.; McClellan, M. R.; Sayers, M. J.; Gay, R. R.; McFeely, F. R.; Solomon, E. I. *J. Vac. Sci. Technol.* **1980**, *17*, 1080–1084.

(54) Ueno, A.; Onishi, T.; Tarmaru, K. *Trans. Faraday Soc.* **1971**, *67*, 3585–3589.

(55) (a) Saussey, J.; Lavelley, J.-C.; Lamotte, J.; Rais, T. *J. Chem. Soc., Chem. Commun.* **1982**, 278–279. (b) Lavelley, J.-C.; Saussey, J.; Rais, T. *J. Mol. Catal.* **1982**, *17*, 289–298. (c) Deluzarche, A.; Hindermann, J.-P.; Kieffer, R. *J. Chem. Res., Synop.* **1981**, 72–73.

(56) Sonnenberger, D. C.; Marks, T. J., manuscript in preparation.